MASTERARBEIT

Titel der Masterarbeit

EGFR-dependent epigenetic aspects of epithelial tumorigenesis

verfasst von

Elena Schmidt BSc

angestrebter akademischer Grad

Master of Science (MSc)

Wien, 2013

Studienkennzahl lt. Studienblatt:	A 066 830
Studienrichtung lt. Studienblatt:	Masterstudium Molekulare Mikrobiologie und Immunbiologie
Betreut von:	Prof. Dr. Christian Seiser

Durchgeführt an der Medizinischen Universität Wien, Institut für Krebsforschung, Innere Medizin I, Abteilung molekulare und zelluläre Tumorbiologie, angewandte und experimentelle Onkologie unter der Leitung von Univ. Prof. Dr. Maria Sibilia und der Betreuung durch Dr. Fabio Savarese.

Acknowledgements

Table of content

1 Introduction

1.1 Epigenetics and cancer

The term epigenetics was first introduced in 1942 by Conrad Waddington (Waddington, 2012). Nowadays, a consensus definition of epigenetics summarizes it as heritable phenotypic variations which are not based on mutations in the primary DNA sequence (Jaenisch and Bird, 2003). Epigenetic mechanisms are mediated by changes in the chromatin configuration (Jenuwein and Allis, 2001). It is possible to distinguish between activating histone marks, associated with actively transcribed genes, (e.g. H3 lysine 4 tri-methylation (H3K4me3)), repressive histone marks, found at inactive loci (e.g. H3 lysine 27 tri-methylation (H3K27me3)) (Lee et al., 2010) and DNA methylation, which is considered as the strongest inhibitory chromatin mark (Wu and Zhang, 2010). Moreover, non-coding RNA, histone variants and chromatin remodeling are as well considered to be part of the epigenetic gene regulation and are known to be heritable from one to the next generation (Chong and Whitelaw, 2004; Liu Liang, 2008). In recent years, novel sequencing techniques have allowed to monitor the epigenetic patterns on a genome-wide scale, resulting in the elucidation of cellular epigenomes (Bock and Lengauer, 2008; Metzker, 2010; Reis-Filho, 2009).

For decades, genetic mutations were considered to exclusively initiate and perpetuate the process of tumorigenesis (Weber et al., 2007). However, recently it was shown that gene activation as well as inactivation via epigenetic mechanisms is also important in the process of tumor progression (Esteller, 2007; Hanahan and Weinberg, 2011). Epigenetic gene regulation impacts on the cellular identity and is often dysregulated in cancer (Berdasco and Esteller, 2010). In contrast to genetic mutations, epigenetic mutations are reversible, which makes them an attractive target for therapeutic approaches. So far, several chromatin remodeling enzymes, such as DNA- and histone-methyltransferases have been identified as oncogenes. The aberrant function of these genes leads to the inactivation of entire sets of genes in tumor cells (Esteller, 2007; Lujambio and Esteller, 2009; Ting et al., 2006). The biochemical functions of "epigenetic" oncogenes such as the H3K27me3 specific histone methyltransferase Ezh2 (Ezhkova et al., 2009) are now increasingly understood. However, relatively little is known about their role in the development of cancer. Thus, efforts are needed to better understand epigenetic mechanisms and their contribution to tumorigenesis in molecular detail. With

regard to head and neck squamous cell carcinoma (HNSCC) research results have shown that epigenetic modifications, especially DNA methylation have a relevant factor in disease progression (Chaisaingmongkol et al., 2012). Accordingly, Weber et al. (2007) could show the hypermethylation of tumor suppressor genes in pre-stage HNSCC. Therefore, epigenetic modifications could serve as "biomarkers" for early detection of HNSCC. DNA methylation is reversible by DNA demethylating agents. In several studies, a reduction in proliferation (Koutsimpelas et al., 2012) as well as an increase in apoptosis (Zhao et al., 2013) in tumor cell cultures could be shown after the treatment with DNA demethylating agents. These results display an interesting starting point for novel, purposeful therapies.

1.2 The Epidermal growth factor receptor (EGFR)

The epidermal growth factor receptor (EGFR) pathway is one of the best studies RTK signaling networks, with a plethora of roles both in development as in disease (Sibilia et al., 2007). The EGFR (ERBB1/HER1) is a glycoprotein of 170 kDa, which is encoded on chromosome 7p12 (Davies et al., 1980). The EGFR family consists of several tyrosine kinase receptors that are structurally related to the EGFR and include ERBB2/HER2/Neu, ERBB3/HER3 and ERBB4/HER4 (Schlessinger, 2002). The four receptors share a common structure with an extracellular ligand-binding domain (domains I, II, III, IV), a single membrane-spanning region as well as a tyrosine kinase domain in the cytoplasma which is flanked by a carboxy terminal tail with containing tyrosine autophosphorylation sites (Citri and Yarden, 2006; Yarden and Sliwkowski, 2001). HER receptors are predominantly found in cells of epithelial, mesenchymal and neuronal origin (Wheeler et al., 2010). ERBB1 and ERBB4 are fully functional receptors and can function as homo- or heterodimers. In contrast to that, ERBB2 lacks a ligand-binding domain and ERBB3 lacks its intrinsic tyrosine kinase activity, giving its necessity to heterodimerize with a signaling competent member of the ERBB family for signal transduction (Sharif and Prevot, 2010)(Figure 1). Until now, seven ligands are known to be able to bind to the receptor: amphiregulin (AR), betacellulin (BTC), heparin-binding EGF-like growth factor (HB-EGF), transforming growth factor α (TGFα), epiregulin (EREG), epigen (EPGN) and epidermal growth factor (EGF). Binding of EGFR by its natural ligands leads to a conformational change in the receptor, which promotes homodimeriztaion with other EGFR molecules or heterodimerization with other HER

family members (especially HER-2). The dimerization results in subsequent autoactivation of the tyrosine kinase on the intracellular portion of the receptor. This process activates an intracellular signaling cascade, that ultimately results in downstream consequences of receptor activation, including inhibition of apoptosis, activation of cell proliferation and angiogenesis as well as an increase in metastatic potential (Benavente et al., 2009; Roskoski, 2004). One signaling pathway which is activated through the receptor tyrosine kinase includes phosphatidylinositol-3-kinase/v-AKT, which has long been a target of novel therapies (Cooper et al., 2009). Other signaling cascades which are also activated include the mitogen-activated protein kinase (MAPK), STAT and phospholipase Cγ pathways and result in cell cycle activation (Yarden and Sliwkowski, 2001). The proliferation of tumor cells, their survival, invasion as well as angiogenesis can be promoted by aberrant activation of these pathways (Wheeler et al., 2010), which often results from receptor overexpression, mutation, ligand-dependent receptor dimerization, and ligand-independent activation (Dempke and Heinemann, 2009).
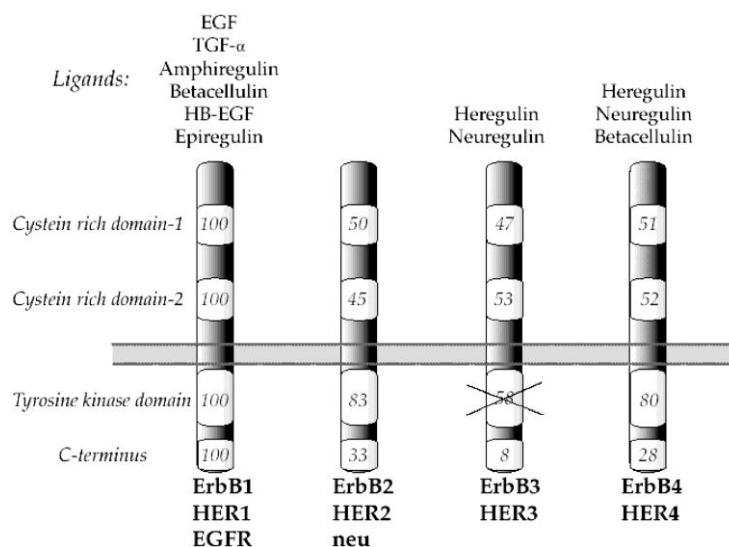
Figure 1: Schematic diagram of the four ErbB family members and their ligands. Adapted from Harari, 2004.

1.3 The role of the EGFR during skin tumorigenesis

The EGFR is a central regulator of proliferation and cell cycle progression and is commonly expressed at high levels in many epithelial tumors (Sibilia et al., 2007). Döbrossy (2005) could show that HNSCC overexpress EGFR in up to 100% of cases, rendering it an interesting target for cancer therapy. Its implication in tumor progression has been extensively studied in a mouse model of epithelial tumors by

transgenic expression of the Ras activator SOS (K5-SOS transgenic mice). Thereby, it has been shown that the EGFR provides an important survival signal to tumor cells whereas tumor cell proliferation is controlled by autocrine VEGF-VEGFR signaling (Lichtenberger et al., 2010; Sibilia et al., 2000). Ligand binding (most often amphiregulin and TGF-α in head and neck cancer) results in homo- or heterodimerization with other family members and subsequent autophosphorylation and activation. Up-regulation of TGF-α and EGFR expression is a hallmark of carcinogenesis in HNSCC (Cooper et al., 2009). Furthermore, high levels of EGFR expression are often correlated with poor prognosis (Wheeler et al., 2010) and resistance to radiation therapy in a variety of cancers, mostly in squamous-cell carcinoma of the head and neck (Zimmermann et al., 2006)**.** Aberrant EGFR activation can thereby lead to enhanced proliferation and other tumor promoting activities. EGFR overexpression is known to be an early event in HNSCC carcinogenesis. When compared to healthy controls, the overexpression is already found in "healthy" mucosa and increases in parallel to histological abnormalities from hyperplasia to invasive carcinoma (Rubin Grandis et al., 1996; Zimmermann et al., 2006).

1.4 Squamous cell carcinoma

Squamous cell carcinoma is the second most common form of skin cancer. It is described as an uncontrolled growth of squamous epithelia, with the epidermis, the skin´s outermost sheath being the most prominent member. This type of cancer mainly results from continuing sun light exposure and is thus thought to be caused by UV irradiation induced DNA damage (Ichihashi et al., 2003).

1.4.1 Head and neck squamous cell carcinoma

Head and neck cancers are the sixth most common malignant tumors in the world (Kamangar et al., 2006) and responsible for approximately 350,000 deaths annually (Ferlay et al., 2010). According to the National Cancer Institute at the National Institutes of health, head and neck cancer is defined as a cancer that arises in the head and neck region including the nasal cavity, sinuses, lips, mouth, salivary glands, throat or larynx (Figure 2). Usually, this type of cancer begins in the squamous cells that line the moist, mucosal surfaces inside the head and neck. HNSCC accounts for over 90% of all head and neck cancers (Batsakis, 1979). The most important risk factors for head and neck cancers are alcohol and tobacco usage, which even seem to have a synergistic effect

(Leemans et al., 2011). These two risk factors are important for cancers of the oral cavity, oropharynx, hypopharynx and larynx (Gandini et al., 2008; Hashibe et al., 2007), but are no risk factors for salivary gland cancers. Furthermore, infection with human papillomavirus (HPV) is a risk factor for some types of head and neck cancers, especially oropharyngeal cancer that involves the tonsils or the base of the tongue. Despite these exogenous risk factors, inherited disorders, such as Fanconi anaemia, but also some kind of genetic susceptibility predispose to HNSCC (Cloos et al., 1996; Hopkins et al., 2008; Kutler et al., 2003). Although an improvement of locoregional control could be achieved, the current survival rates of HNSCC patients remain disappointing. For HNSCC the 5-year survival rate is approximately 50-60% and this value has only increased slightly during the last three decades (Ragin et al., 2007). Head and neck cancers consistently metastasize to distant sites such as the lung or the liver. Treatment for early stage SCC often involves surgery and radiation therapy (RT) whereas locally-advanced tumors are treated with concurrent chemotherapy to RT. In addition, therapies targeting the EGFR have improved the outcome of conventional chemotherapy in pre-clinical as well as clinical studies. Unfortunately, therapies that lead initially to partial response or disease stabilization often result in resistance of the patient against the treatment. Therefore, current research is focused on understanding the molecular mechanisms of the development, the progression as well as resistance mechanisms of HNSCC. This will facilitate the design of novel individualized therapies that may improve survival.

To succeed in understanding these mechanisms, immortalized cell lines are used which are directly isolated from patients with HNSCC tumors and help to understand molecular, biochemical, genetic and immunological properties of this type of cancer in detail.
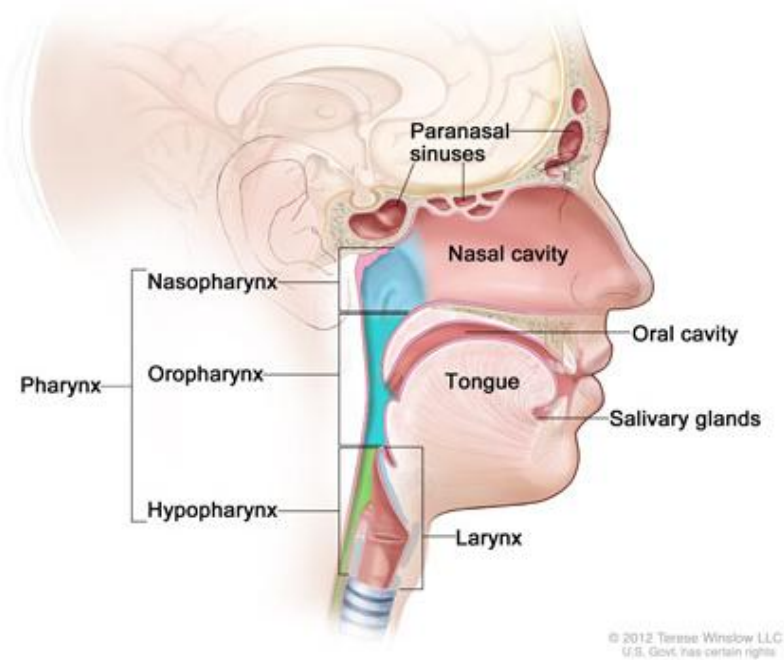
Figure 2: Head and neck cancer regions[1]

1.5 Targeted EGFR inhibitors and resistance mechanisms

During the past decade, intense research has led to the invention of molecular therapeutics, as a new era of cancer treatment. Molecular targeted therapies and predictive biomarkers, used to select patients who especially benefit, promise to further improve outcome (Scully and Bagan, 2009). Due to the deregulation of EGFR signaling in pre-stage HNSCC (Diniz-Freitas et al., 2007; Kalyankrishna and Grandis, 2006), the EGFR is a preferential target for new therapy against this type of cancer, with a broad spectrum of inhibitors currently under investigation (Baselga, 2001). Two complementary therapeutic strategies have been developed and are used to treat patients in the context of controlled clinical trials (Ciardiello and Tortora, 2008; Harari, 2004). The first strategy targets the extracellular domain of the receptor with monoclonal antibodies (e.g. cetuximab (Erbitux) or panitumumab (Vectibix)). This leads to an inhibition of the stimulation of the receptor by endogenous ligands through competitive inhibition and also results in internalization and degradation of the antibody-receptor complex, down-regulating EGFR expression. Furthermore, blocking of the EGFR by a monoclonal antibody results in inhibition of cell proliferation, enhanced

---

[1] http://www.cancer.gov/cancertopics/factsheet/Sites-Types/head-and-neck

apoptosis, reduced angiogenesis, invasiveness as well as metastasis (Zimmermann et al., 2006)**.** As mentioned, one immunoglobulin G1 chimeric human-mouse monoclonal antibody, utilized in this Master´s thesis to develop cell lines with acquired resistance, is cetuximab (Figure 3). In March 2006, cetuximab was approved by the FDA[2] for use in combination with radiation therapy for treating locoregionally advanced HNSCC. Furthermore, cetuximab was approved as a single agent, for cancer treatment in patients with recurrent or metastatic HNSCC, where the platinum-based therapy did not succeed (Wheeler et al., 2010). Despite the functions of cetuximab as a monoclonal antibody, as described above, it can also induce antibody-dependent cell-mediated cytotoxicity (Kimura et al., 2007). The mean half-life of cetuximab is approximately 112 hours in humans (Goldstein et al., 1995; Kawamoto et al., 1983).

The other class of EGFR inhibitors, which are used successfully in cancer treatment, are low-molecular-weight tyrosine kinase inhibitors (TKIs) that target the catalytic domain of the EGFR. TKIs act by inhibiting ligand-induced receptor phosphorylation by competing for the intracellular Mg-ATP-binding site (Ciardiello, 2000; Wheeler et al., 2010)**.** To date, three anti-EGFR TKIs, gefitinib (ZD1839, Iressa), erlotinib (OSI-774, Tarceva) and lapatinib (GW572016, Tykerb) have been approved by the FDA for use in oncology (Brand et al., 2011a). Another TKI which is undergoing Phase II clinical trials for head and neck cancer is afatinib (BIBW-2992, planned trade name Tomtovok, previously Tovok)[3]. However, afatinib is not a first-line treatment and is only used after other therapies have failed. In addition to these treatments, Twigger et al. (2012) could show that reoviral killing exerts potent oncolytic effects in head and neck cancer cell lines independent of EGFR signaling. Although, there is great clinical promise, since up to 20% of cancer patients respond to the EGFR inhibition, the majority of the patients develop either intrinsic or acquired resistance to EGFR inhibitor treatments (Arteaga, 2003; Bianco et al., 2005; Engelman and Jänne, 2008; Viloria-petit and Kerbel, 2004; Wheeler et al., 2010). As described by Dempke and Heinemann (2009) there are several general processes which are known to lead to molecular mechanisms of resistance. These include activation of alternative tyrosine kinase receptors that bypass the EGFR pathway (e.g. IGF-1R and c-MET), increased angiogenesis, constitutive activation of downstream mediators such as PTEN or K-ras and the occurrence of specific EGFR

---

[2] http://www.cancer.gov/clinicaltrials/results/summary/2010/head-neck-cetuximab0604
[3] http://www.clinicaltrials.gov/show/NCT01345669

mutations. Furthermore, multiple resistance mechanisms towards cetuximab have been found (Brand et al., 2011b). However, the investigation of epigenetic effects on drug resistance is the center of recent research (Rosenzweig, 2012) to identify novel targets for therapeutic intervention.
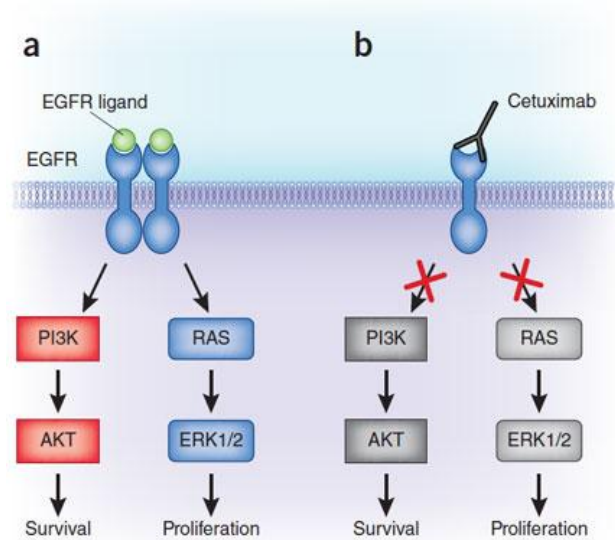
Figure 3: Binding of cetuximab to EGFR. (a) Binding of EGFR ligands to the extracellular domain of EGFR leads to receptor dimerization and activation of downstream signaling cascades, resulting in cell survival or proliferation. (b) Binding of cetuximab to EGFR blocks binding of other ligands, resulting in the inhibition of downstream signaling cascades, and prevents the survival and proliferation of tumor cells. Adapted from Bardelli and Jänne, 2012.

1.6 Vascular endothelial growth factor (VEGF) pathway

Vascular endothelial growth factor receptors (VEGFRs) are tyrosine kinase receptors which regulate the cardiovascular system (Olsson et al., 2006). During embryogenesis, VEGFs are crucial regulators of the vascular development (vasculogenesis), whereas in the adult they induce blood-vessel formation (angiogenesis) (Olsson et al., 2006). In mammals, five VEGF ligands (VEGF A, B, C, D and placenta growth factor (PLGF)) have been identified so far (Cursiefen et al., 2004). VEGFA is a potent growth factor which is a ligand for the tyrosine kinase receptors VEGFR1 (Flt-1) and VEGFR2 (KDR/Flk-1). PLGF and VEGF-B bind only to VEGFR1, whereas VEGF-C and VEGF-D bind to VEGFR2 and VEGFR3 (Carmeliet, 2003). However, VEGFR2 is thought to be more important in tumor angiogenesis and vasculogenesis. Inhibition of VEGFR2 (but not VEGFR1) was shown to prevent angiogenic switching, persistent angiogenesis and initial tumor growth (Dempke and Heinemann, 2009). Kyzas et al. (2005) could show in a meta-analysis of 1002 HNSCC patients that increased expression of VEGFA was associated with bad

prognosis. Another ligand which is very important and thought to mediate lymphangiogenesis is VEGFC which acts on VEGFR3 (Flt-4) (Joukov et al., 1996). In a study of 60 HNSCC patients it was shown that VEGFC expression correlates with lymph node metastasis (Kyzas et al., 2005a). Different strategies have been developed to target VEGFR-signaling. However, the most successful one, which was approved by the FDA in 2004, is the VEGF-neutralizing antibody bevacizumab/avastin. Other inhibitors, known to target the VEGF/VEGFR pathways comprise soluble VEGFRs, receptor tyrosine-kinase inhibitors (RTKI) as well as neutralizing aptamers. Two kinase inhibitors, Sorafenib and Sunitinib, have been tested in large phase III clinical trials and are showing promising results as monotherapies (Olsson et al., 2006). Thus, the VEGF pathway is also a promosing target in cancer therapy. Unfortunately, similar to EGFR-inhibition, agents that selectively target VEGFR2 or VEGF initially showing promising activity in clinical trials, always lead to resistance in the cancer patients after a certain time. So far, pre-clinical studies have begun to uncover mechanisms of resistance to anti-angiogenetic drugs, which comprise upregulation of bFGF, overexpression of MMP-9, increased levels of SDF-1α and HIF-1α-induced recruitment of bone marrow-derived CD45+ myeloid cells (Dempke and Heinemann, 2009). Thus, as with respect to the EGFR, efforts to understand how patients develop resistance to the treatment are greatly needed.

2 Aims of the thesis

The aim of my Master´s thesis was to identify gene expression patterns associated with acquired resistance to the epidermal growth factor receptor (EGFR)-inhibitor cetuximab and in particular whether epigenetic changes are associated with these in epithelial tumors such as squamous cell carcinomas (SCC). By developing cetuximab-resistant head and neck SCC cell lines from initially cetuximab-sensitive ones, I wanted to address the changes cells undergo upon developing resistance against cetuximab and gain new insights into the cellular and molecular consequences of acquired cetuximab resistance. I addressed whether cetuximab-induced reduction of cell growth results from increased apoptosis, inhibition of cell proliferation or both and if the cell lines keep their proliferative potential *in vivo*. Whole-genome bisulfite sequencing (WGBS) brought insight whether loss or gain of global DNA methylation is necessary to develop resistance, providing additional information about the consequences of cetuximab resistance on gene expression. By performing RNA Sequencing, I tested which changes in the transcriptomes are associated and potentially causative of the acquired resistance to cetuximab and if I could find candidate genes which may be useful as biomarkers. The up-regulation of the vascular endothelial growth factor A (VEGFA) in cetuximab-resistant cell lines, led us to analyze what effects VEGFA has on cancer cell proliferation and whether it reduces cetuximab sensitivity in cetuximab-sensitive cell lines.

12

3 Results

3.1 Preliminary characterization of (HN)SCC cell lines

3.1.1 Analysis of the EGFR signaling cascade

The human HNSCC cell lines HNSCC11 and HNSCC22 as well as the SCC cell line SCC13 were used to generate cell lines resistant to the EGFR inhibitor cetuximab. Foremost, we needed to clarify whether the cell lines could actually be used for the process of generating cetuximab-resistant cell lines. To test whether our cell lines responded to inhibition of EGFR, the effect of the dual receptor tyrosine kinase inhibitor (TKI) BIBW 2992 on the EGFR signaling cascade was examined. $1x10^5$ cells of each cell line were seeded in 6-well dishes and exposed to BIBW 2992 (1μM) for 24 h. As a control, cells were cultured in the absence of the inhibitor. After protein isolation, immunoblotting analysis was performed to analyze the downstream EGFR signaling cascade. The experiment showed that all three cell lines responded well to the TKI. Figure 4 indicates that BIBW 2992 effectively blocked the EGFR as all cell lines showed reduced phosphorylation of ERK1/2 and EGFR after treatment with BIBW 2992. This result suggests that the inhibitor affected the EGFR signaling cascade and that the cell lines were applicable for the process of generating cetuximab-resistant cell lines.
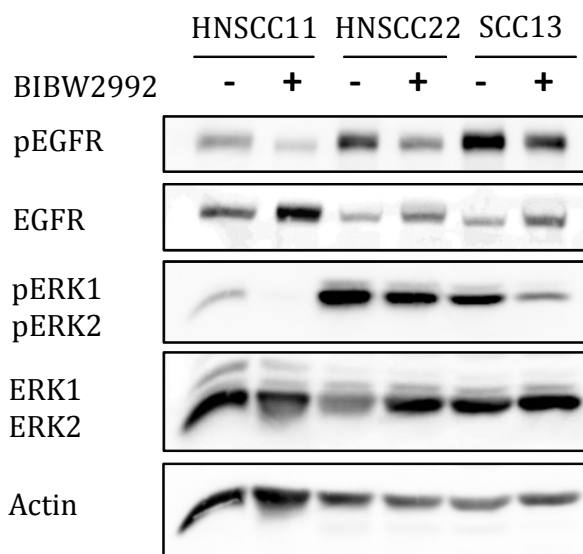
Figure 4: EGFR signaling profile of EGFR inhibitor-sensitive cells. Parental EGFR inhibitor-sensitive cells were exposed to BIBW 2992 (1µM) for 24 h. As a control, cells were cultured without exposure to the inhibitor. After harvesting, cells were lysed and processed for immunoblotting using antibodies directed against pEGFR, EGFR, pERK1/2 and ERK1/2. Actin served as a loading control.

Next, the inhibitory potential of cetuximab on the EGFR signaling cascade was investigated in the respective (HN)SCC cell lines. The receptor inhibition was examined by seeding the cells in 6-well plates and culturing them under different conditions. $1x10^5$ cells were cultured under starvation conditions for 24 h. After the inhibition with different concentrations of cetuximab (10 µg/ml, 100 µg/ml, 1000 µg/ml) for 1 h, stimulation with EGF (250x) followed for 20 min. As controls, cells were cultured (1) under normal conditions w/o treatment, (2) under starvation conditions w/o treatment and (3) under starvation conditions, stimulated with EGF and w/o cetuximab pre-treatment. After 24 h, cells were harvested, lysed and processed for immunoblotting. Western blot analysis (Figure 5) revealed that the strongest signal of ERK1/2 as well as EGFR phosphorylation was seen in cells cultured under starvation conditions and stimulated with EGF (w/o pre-treatment of cetuximab). Furthermore, cetuximab effectively blocked the EGF-stimulated activation of EGFR in a dose-dependent manner, as can be seen with regard to the decreasing phosphorylation of ERK1/2 and EGFR with increasing concentrations (a, b, c) of cetuximab. Therefore, I conclude that the EGFR is not mutated in the cell lines and responds normally after stimulation with its natural ligand.
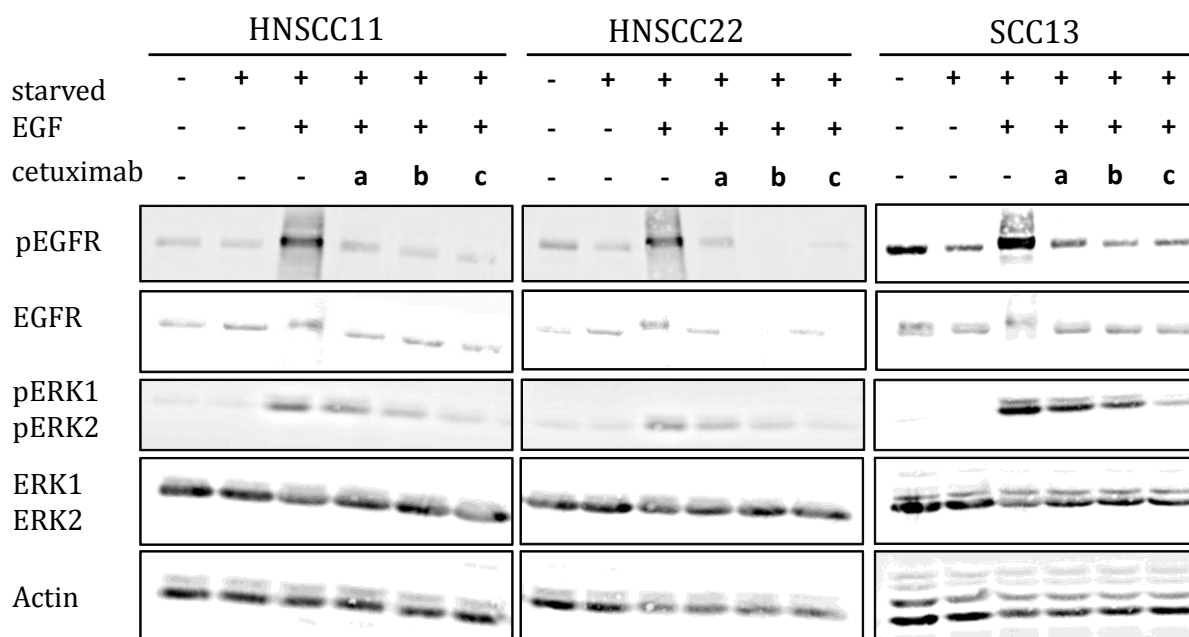
Figure 5: EGFR signaling profile of EGFR inhibitor-sensitive cells. Parental cells were cultured under starvation conditions for 24 h and exposed to different concentrations of cetuximab (a = 10 µg/ml, b = 100 µg/ml, c = 1000 µg/ml) for 1 h followed by 20 min of EGF stimulation. As controls, cells of the respective cell lines were cultured under normal conditions w/o treatment, in starvation medium w/o treatment as well as under starvation conditions with stimulation of EGF (w/o pre-treatment of cetuximab). After harvesting, cells were lysed and processed for immunoblotting using antibodies directed against pEGFR, EGFR, pERK1/2 and ERK1/2. Actin served as a loading control.

3.1.2 Gene expression analysis

The results presented so far indicated that all cell lines were good candidates for the generation of resistant cells, based on the successful inhibition of the EGFR signaling cascade by cetuximab. To get a clearer picture about the EGFR inhibitor-sensitive cells, a gene expression analysis by using real-time PCR was performed including the following genes: *EZH1* and *EZH2* are both histone-lysine-N-methyltransferases and cogovern H3K27 trimethylation. *JUN*, in combination with *FOS* and *FOSB* forms the AP-1 early response transcription factor. In addition, *FOS* is known to be a cellular proto-oncogene. *MYC* is a regulator gene and codes for a transcription factor. Interestingly, a mutated version of *MYC* is found in many cancers, causing it to be constitutively expressed. *UTX* and *JMJD3* are both histone H3K27 demethylases involved in HOX gene regulation and development. *DNMT1*, or DNA (cytosine-5-)-methyltransferase 1, is the maintenance DNA methyltransferase and is involved in the establishment and regulation of tissue-specific patterns of methylated cytosine residues. It is known that aberrant methylation patterns are associated with several human tumors. Thus, *DNMT1* is a potent oncogene

(Esteller, 2007). *SU(VAR)3-9* encodes a histone methyltransferase (HMTase) which selectively methylates histone H3 at lysine 9 (H3-K9) (Schotta et al., 2002). Figure 6 shows the relative expression levels of all analyzed genes in the (HN)SCC cell lines HNSCC11, SCC13 and HNSCC22. The relative gene expression of all analyzed genes, with the exception of the genes *EZH2*, *DNMT1* and *SU(VAR)39*, was stronger in the cell line SCC13 compared to the HNSCC cell lines. In contrast to that, the HNSCC cell lines compared with each other showed nearly the same expression levels of the indicated genes. Interestingly, the expression of EGFR was nearly 2-fold higher in the cell line SCC13 compared to the HNSCC cell lines. This result suggests that the indicated genes are expressed in all cell lines and that the relative gene expression levels in the HNSCC cell lines are more similar compared with each other than with the SCC cell line SCC13.
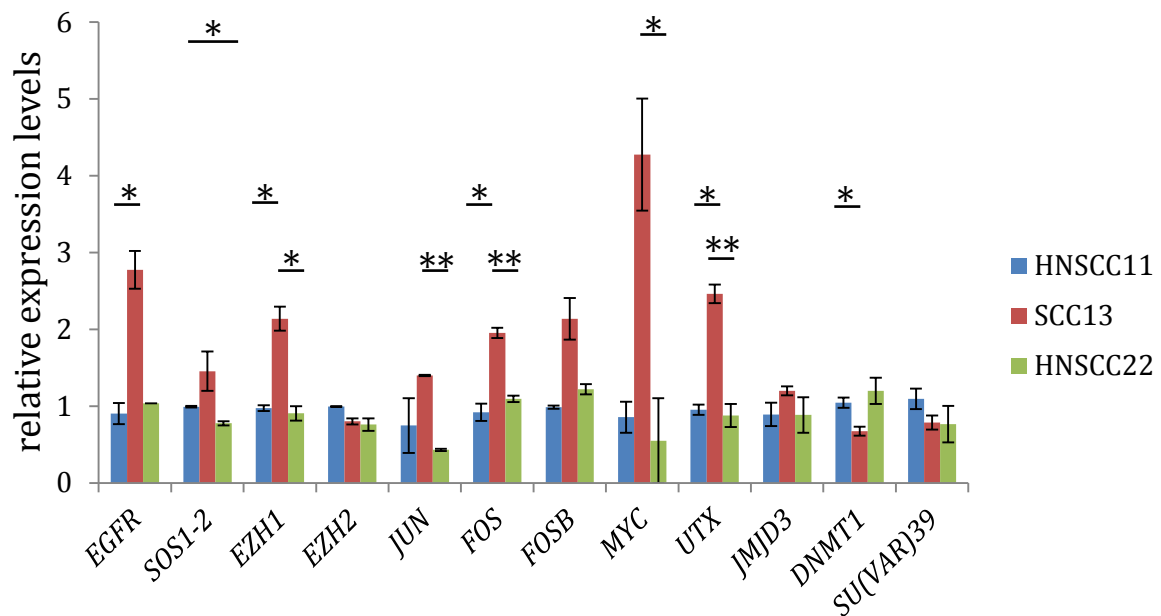
Figure 6: Relative expression levels of *EGFR, SOS1-2, EZH1, EZH2, JUN, FOS, FOSB, MYC, UTX, JMJD3, DNMT1* and *SU(VAR)39* in EGFR inhibitor-sensitive (HN)SCC cell lines HNSCC11, SCC13 and HNSCC22. Data represent mean of technical replicates ± SD. * indicates significance (* p≤0,05; ** p≤0,001).

After the preliminary characterization of the cell lines, the cell line HNSCC11 was excluded from the study due to delayed growth.

3.1.3 Analysis of apoptosis after cetuximab exposure

It is known that blocking the EGFR by a monoclonal antibody leads to inhibition of cell proliferation as well as enhanced apoptosis (Zimmermann et al., 2006). This raised the question which effect cetuximab had on the cancer cells which I used in this study. In order to test whether one explanation for the decreased cell count after cetuximab exposure was apoptosis, an apoptosis assay with Annexin V and 7´AAD as well as a TUNEL staining was performed according to Materials and Methods. For both experiments, cells were exposed to cetuximab (40 µg/ml) for 24 h and 48 h. Figure 7 shows that nearly all cells in the positive control undergo apoptosis as the cells are FITC-positive (Figure 7 B and C). The negative control revealed no FITC-positive cells (Figure 7 E and F), indicating that the staining was performed successfully. The staining of the cetuximab treated cells (Figure 7 G, H, I, J, K, L) revealed no FITC-positive cells. From this experiment I conclude that cetuximab does not lead to apoptosis after 24 h and 48 h of cetuximab exposure.
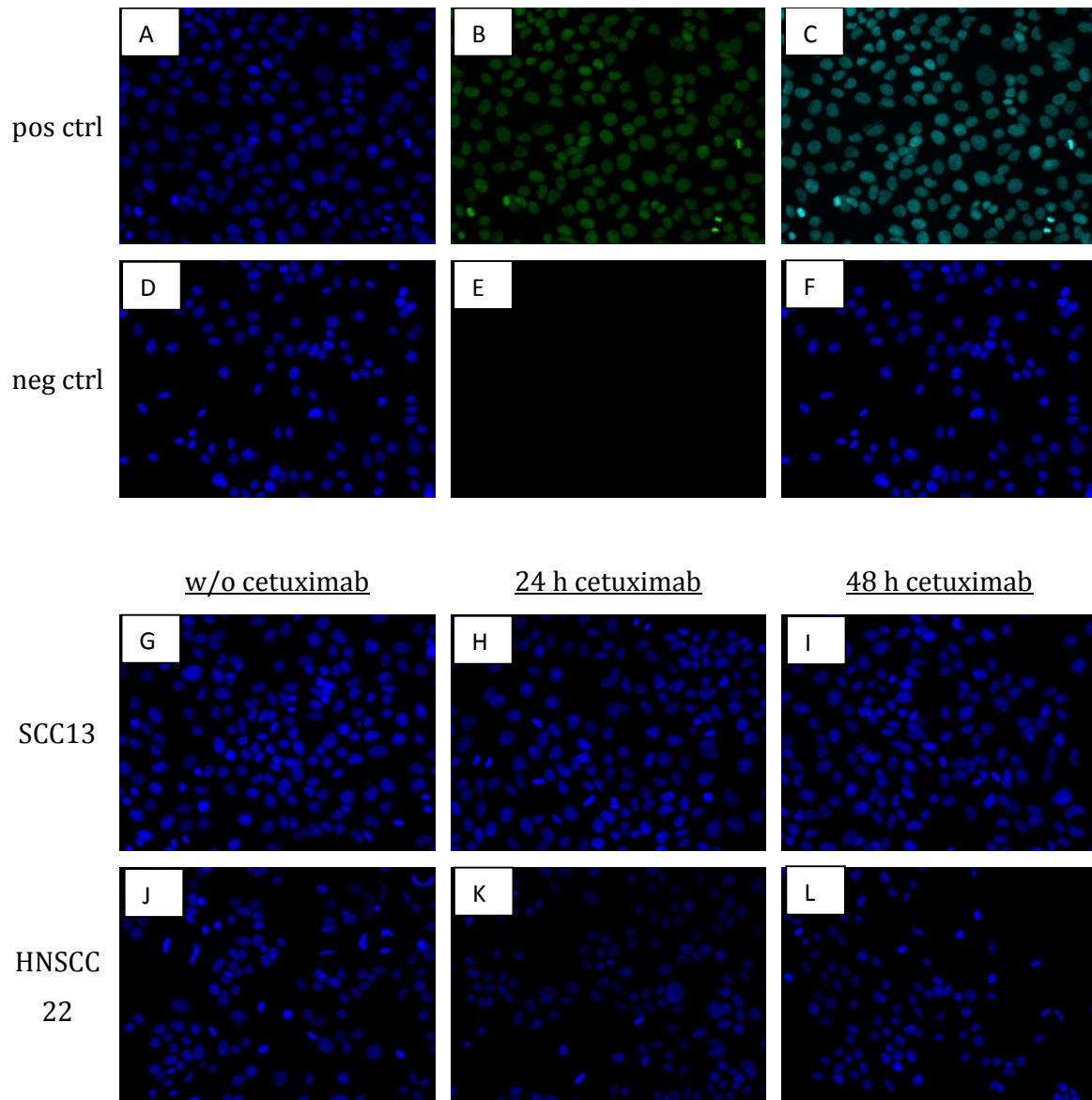
Figure 7: Cetuximab does not induce apoptosis in (HN)SCC after 24 h and 48 h of treatment. A, B, C: positive control; D, E, F: negative control; G, H, I: SCC cell line SCC13 untreated, 24 h treatment and 48 h treatment with cetuximab; J, K, L: HNSCC cell line HNSCC22 untreated, 24 h treatment and 48 h treatment with cetuximab. Images were taken at a magnification of 20X.
A, D – Blue: Hoechst
B – Green: FITC positive
C – Blue: Hoechst, Green: FITC positive
E – FITC negative
F, G, H, I, J, K, L – Blue: Hoechst, FITC negative

In order to support the result of the TUNEL assay, Annexin V and 7´AAD staining was performed. Again, the apoptotic response of the parental (HN)SCC cell lines after cetuximab treatment was investigated. Figure 8 shows the change of early (a) and late (b) apoptotic cell populations between cetuximab untreated as well as cetuximab treated cells after 24 h and 48 h of cetuximab exposure. The cell line HNSCC22 showed a

slight increase in early-apoptosis after 24 h and 48 h of cetuximab exposure. This was also shown for the cell line SCC13 after 48 h of cetuximab treatment, in which the increase was significant (p=0,02). However, after 24 h, there was a slight decrease of early apoptosis in the cetuximab treated cell line SCC13. The analysis of the late apoptosis showed an increase in apoptosis for the cell line SCC13 at both time points, whereas cell line HNSCC22 decreased at these time points. Ultimately, the result strengthened the conclusion from the TUNEL staining, indicating that the decreased cell count after cetuximab exposure for 24 h and 48 h in cetuximab-sensitive cells did not result from late stage apoptosis. From these results I conclude that the decrease in cell growth after cetuximab exposure does not result from late-stage apoptosis.

a

b
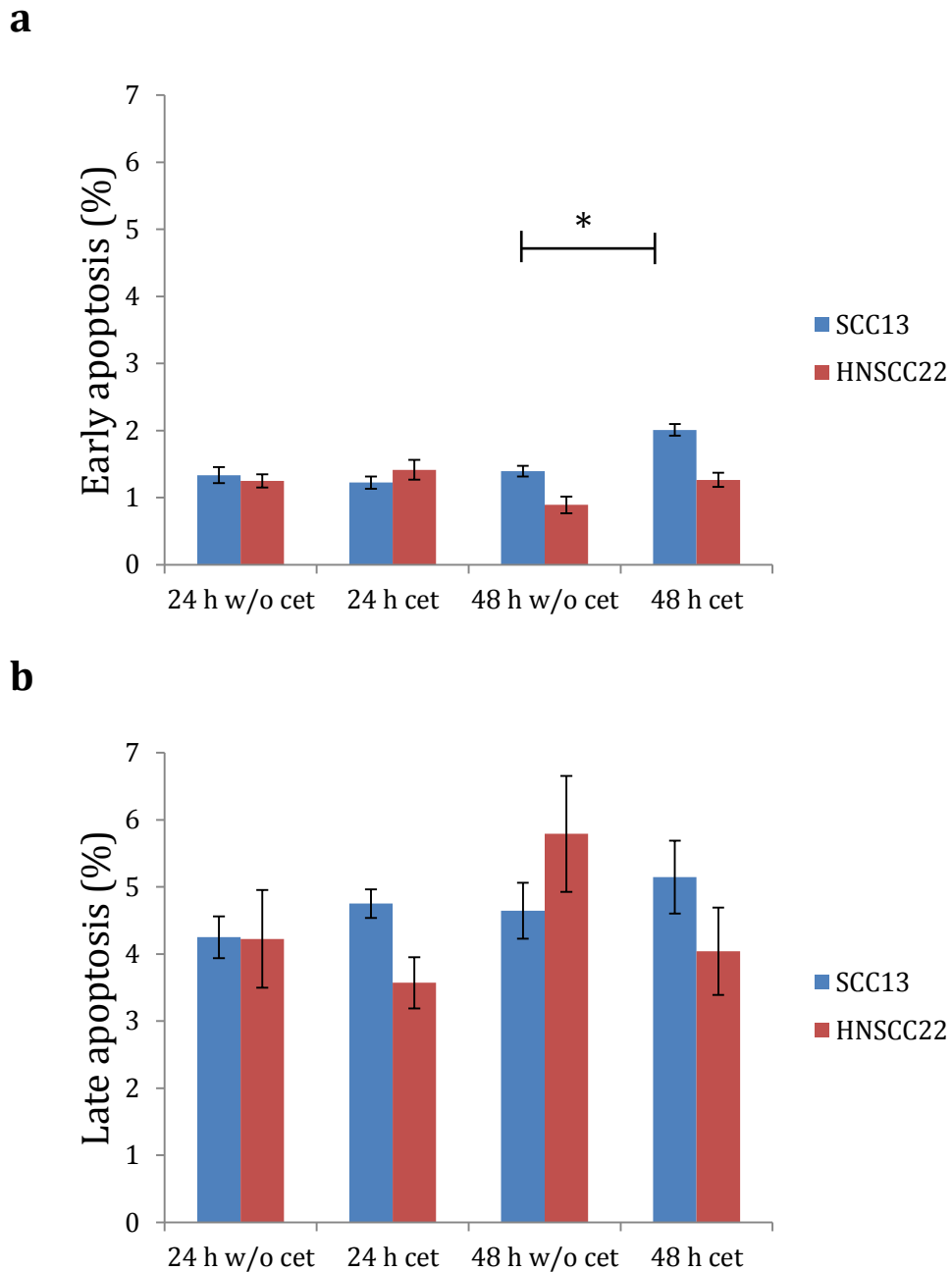
Figure 8: Apoptotic response of (HN)SCC cells following cetuximab exposure. Apoptosis was examined by flowcytometry using AnnexinV and 7´AAD staining as described in Materials and Methods. Parental EGFR inhibitor-sensitive cells (SCC13, HNSCC22) were exposed to cetuximab (40µg/ml) for 24 h and 48 h. The percentage of cells in early (a) and late (b) apoptotic population was analyzed by Cell Quest software (Becton Dickinson). Data represent mean of biological duplicates ± SD. * indicates significance (p≤0,05).

3.1.4 Influence of cetuximab on cell proliferation

The results presented so far argue that other mechanisms than late-stage apoptosis have to be the reason for cetuximab-induced reduction of cell viability. This led us to question whether cetuximab inhibits cell proliferation in the cell lines. In order to test the inhibitory effect of cetuximab on the proliferation rate of sensitive (HN)SCC cell lines, an EdU cell proliferation assay was performed. Thereby, DNA synthesis was measured. EdU (5-ethynyl-2´-deoxyuridine) is a nucleoside analog to thymidine and is incorporated into DNA during active DNA synthesis. For proliferation analysis, 40% confluent cells were incubated with cetuximab (40 µg/ml) for 48 h before pulsing with 5 µM EdU for 8 h and 16 h. Cells were harvested, stained and analyzed on a LSR-II Flow cytometer. Figure 9 shows the quantification of proliferating (HN)SCC cells w/o treatment as well as after treatment with cetuximab. The result showed that more cells incorporated EdU into the DNA over a growth phase of 16 h in contrast to 8 h. Cetuximab exposure for 48 h resulted in significantly reduced proliferation (p=0,02) in the cell line SCC13 compared to the untreated cell line over a growth period of 16 h (Figure 9a). In contrast to that, no difference in proliferation was observed over a growth period of 8. With regard to the cell line HNSCC22, treatment with cetuximab did not result in decreased proliferation over a growth period of 8 h and 16 h. From these results I conclude that cetuximab can have an inhibitory effect on the proliferation of the cell line SCC13.

a
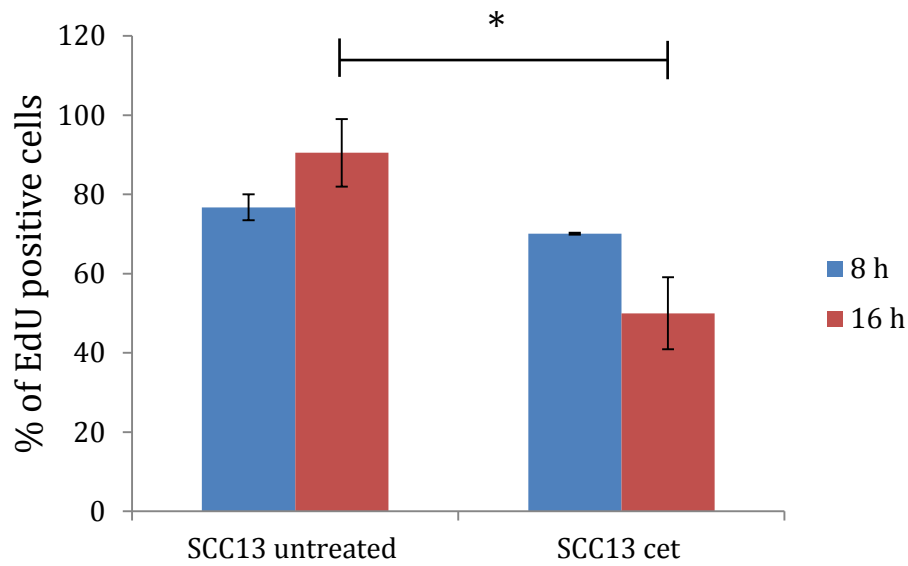
b
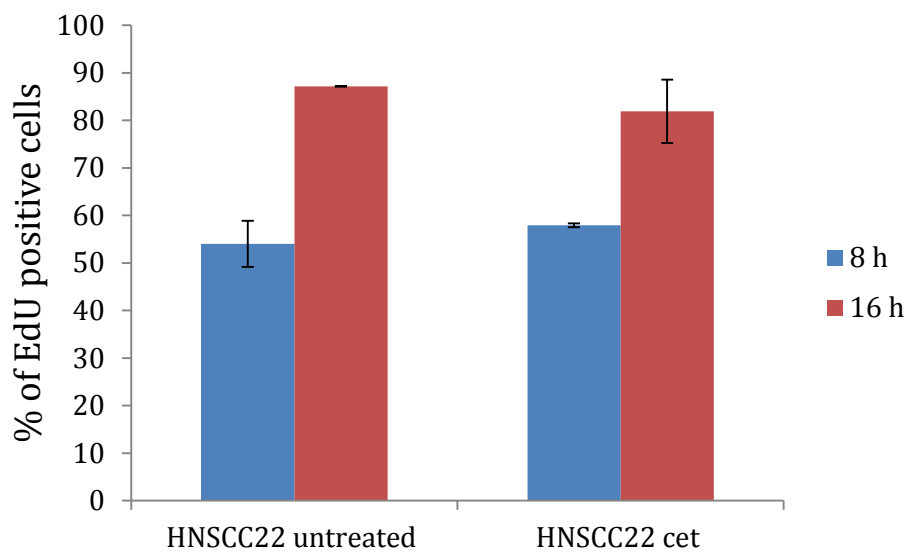
Figure 9: Quantification of proliferating (HN)SCC cells after treatment with cetuximab. Cells of the (HN)SCC cell lines SCC13 (a) and HNSCC22(b) at 40% confluence were left untreated or exposed to cetuximab (40 μg/ml) for 48 h. EdU was added to the culture medium for 8 h and 16 h. Data represent mean of biological triplicates ± SD. * indicates significance (p≤0,05).

3.2 Generation and characterization of cetuximab-resistant (HN)SCC cell lines

3.2.1 Generation of cetuximab-resistant (HN)SCC cell lines

Starting with several, initially cetuximab-sensitive, (HN)SCC cell lines I managed to generate cetuximab-resistant lines by culturing the original cells for multiple passages in the presence of increasing concentrations of cetuximab. Initially, the $IC_{50}\%$[4] value of cetuximab was determined, with which the process of developing EGFR inhibitor-resistant cell lines should be started. In order to measure the relative cell count over a time period of 48 h, two MTT assays were performed, in which the cells were exposed to cetuximab and BIBW 2992 (as a control). 5x 10^3 cells were seeded in a 96-well dish and treated with increasing concentrations of cetuximab (0,1 µg/ml, 1 µg/ml, 10µg/ml and 100 µg/ml) for 48 h. After that, the protocol was performed, analogous to the instructions of the MTT assay kit. Figure 10 shows the effect of the inhibition by BIBW 2992 which was stronger than the effect of cetuximab, as the relative cell viability of the cell lines at the highest concentration of 100nM was around 0,5 to 1,0 whereas the relative cell viability with cetuximab was around 1,0 to 1,5. Nevertheless, all cell lines showed reduced growth, after exposure to increasing concentrations of cetuximab. This result strengthened the preliminary results from the proliferation analysis, showing that cetuximab had an effect on the proliferation of the cells. According to the result from the MTT assay, two different initial concentrations of cetuximab (2,5 µg/ml and 5 µg/ml) were chosen to start the treatment. The exposure dose was doubled every 2nd cell passage until the maximal concentration had been reached. The cetuximab-resistant cell lines (SCC13 R and HNSCC22 R) were treated with a maximal dose of up to 40 µg/ml of cetuximab. These results suggest that the inhibitory effect of BIBW 2992 is stronger than the effect of cetuximab and that the $IC_{50}\%$ value of cetuximab is between 1 µg/ml and 10 µg/ml of cetuximab.

---

[4] half maximal inhibitory concentration, which indicates the measure of the effectiveness of a compound in inhibiting biological or biochemical function

a

b
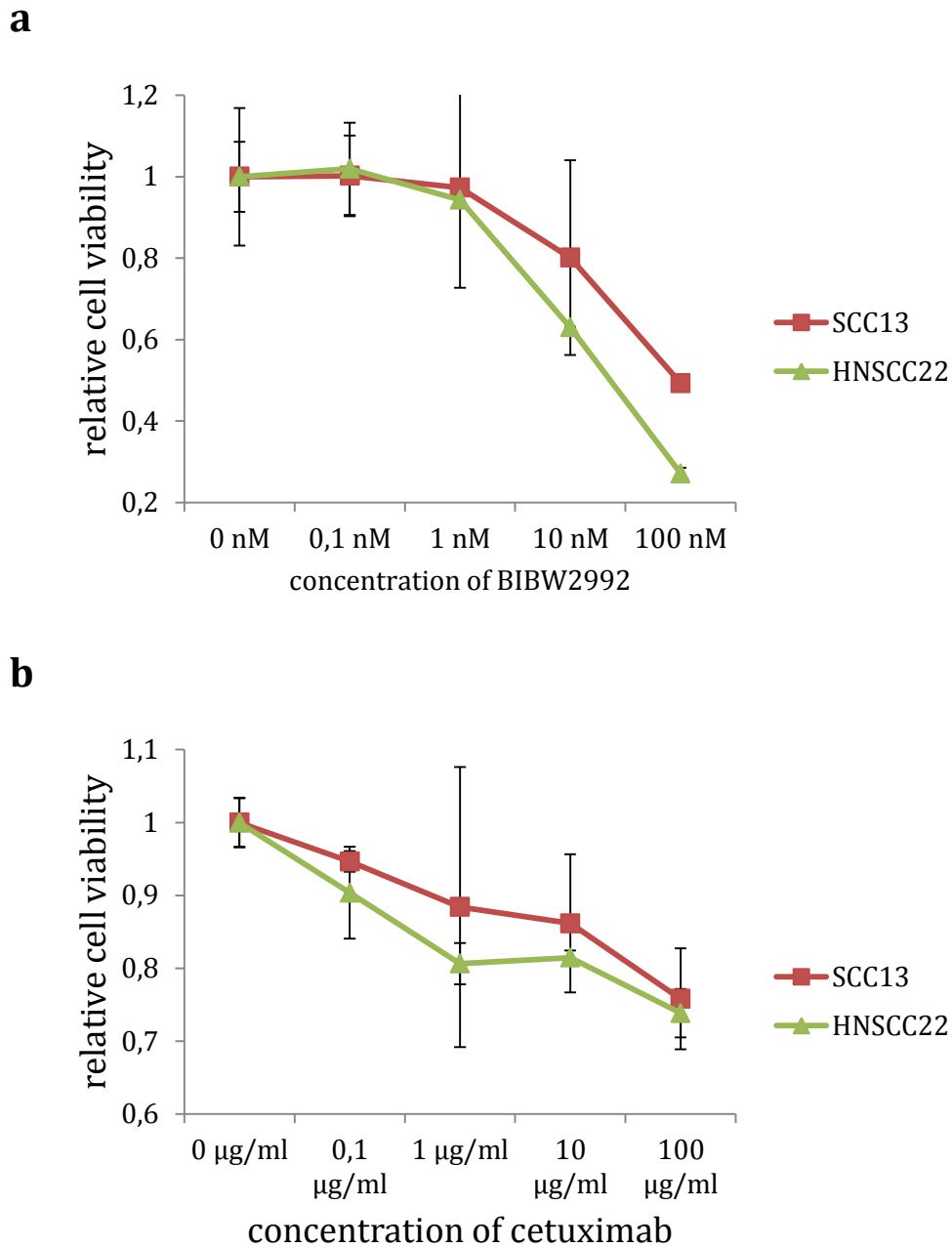
Figure 10: Survival curves of the SCC cell line SCC13 and the HNSCC cell line HNSCC22. The cells were cultured and treated with BIBW 2992 (a) and cetuximab (b) for 48 hours. Afterwards, a MTT proliferation analysis was performed. Data represent mean of biological duplicates ± SD.

During the process of generating cetuximab-resistant cells, MTT assays and immunoblotting analyses (Figure 12), were performed at different time points to confirm the resistance. Finally, after 7 months of treatment (corresponding cell passage 14), the resistance of the cell lines (SCC13 R and HNSCC22 R), cultured with increasing concentrations of cetuximab, was confirmed. The resistance of the cell lines was confirmed by a MTT assay, comparing the relative cell viability of untreated cells with those being exposed to different concentrations of cetuximab. Figure 11 shows the relative cell viability of the resistant cell lines SCC13 R and HNSCC22 R compared to their sensitive counterparts SCC13 S and HNSCC22 S. Both assays revealed an insensibility of the resistant cell lines regarding the inhibitory effect of cetuximab on the cell viability. Hence, the cell lines showed a constant growth rate with increasing concentrations of cetuximab. In contrast to that, the assay revealed that the relative cell viability of the cetuximab-sensitive cell lines decreased with increasing concentrations of the inhibitor. These results show that we had successfully generated cetuximab-resistant cell lines.

a
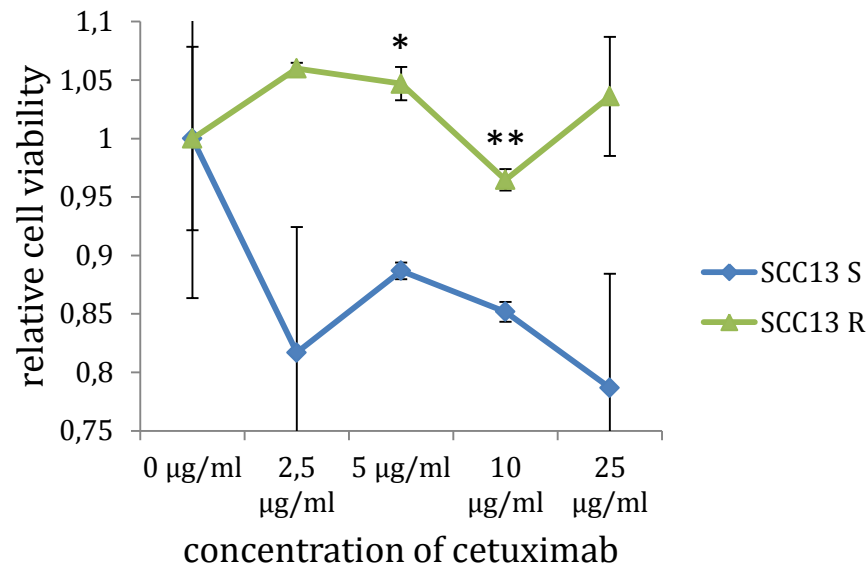
b
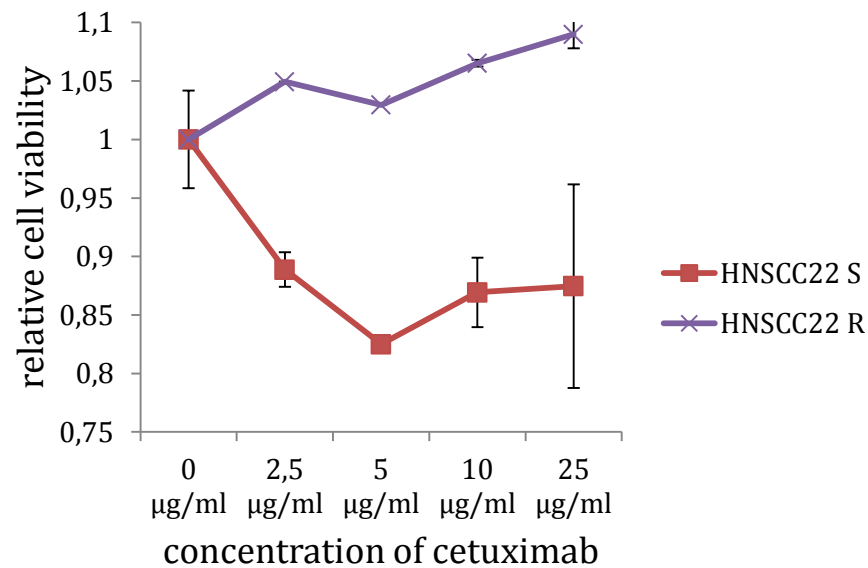
Figure 11: Survival curves of the SCC cell lines SCC13 S and SCC13 R (a) as well as of the HNSCC cell line HNSCC22 S and HNSCC22 R (b). The cells acquired resistance to the EGFR-inhibitor cetuximab by continuous culture in the presence of increasing concentrations of cetuximab. Enclosed from both cell lines, cells were cultured without cetuximab and kept sensitive to the inhibitor. Data represent mean of biological duplicates ± SD. * indicates significance (* p≤0,05; ** p≤0,001).

3.2.2 Analysis of the EGFR signaling cascade in cetuximab-sensitive and -resistant cell lines

During the establishment of cetuximab-resistant cell lines, the cells were characterized in different experiments. In order to confirm the resistance also on the protein level and to gain a first insight into the molecular nature of acquired cetuximab resistance an immunoblot analysis of the SCC cell line 13 (SCC13 S and SCC13 R) was performed. At this time point the cells were treated with a cetuximab concentration of up to 20 μg/ml. For the analysis the cells were treated under different conditions, as described before (3.1.1). I analyzed the phosphorylation of ERK1/2 to determine whether the EGFR signaling cascade was altered in the cetuximab resistant cell lines. By performing immunoblotting analysis of the resistant cell line SCC13 R in comparison with its sensitive counterparts, I observed that treatment with cetuximab effectively blocked the EGF-stimulated activation of EGFR in a dose-dependent manner in the parental sensitive cell line but not in the cetuximab resistant cells. The resistant cells showed high levels of phosphorylated ERK1/2 upon EGF-stimulation preceeded by cetuximab treatment, whereas the sensitive cells did not (Figure 12). Thus, ERK1/2-phosphorylation is not affected by the presence of cetuximab in the culture medium. This result demonstrates that the system of induced cetuximab resistance leads to distinct molecular mechanisms of drug resistance.
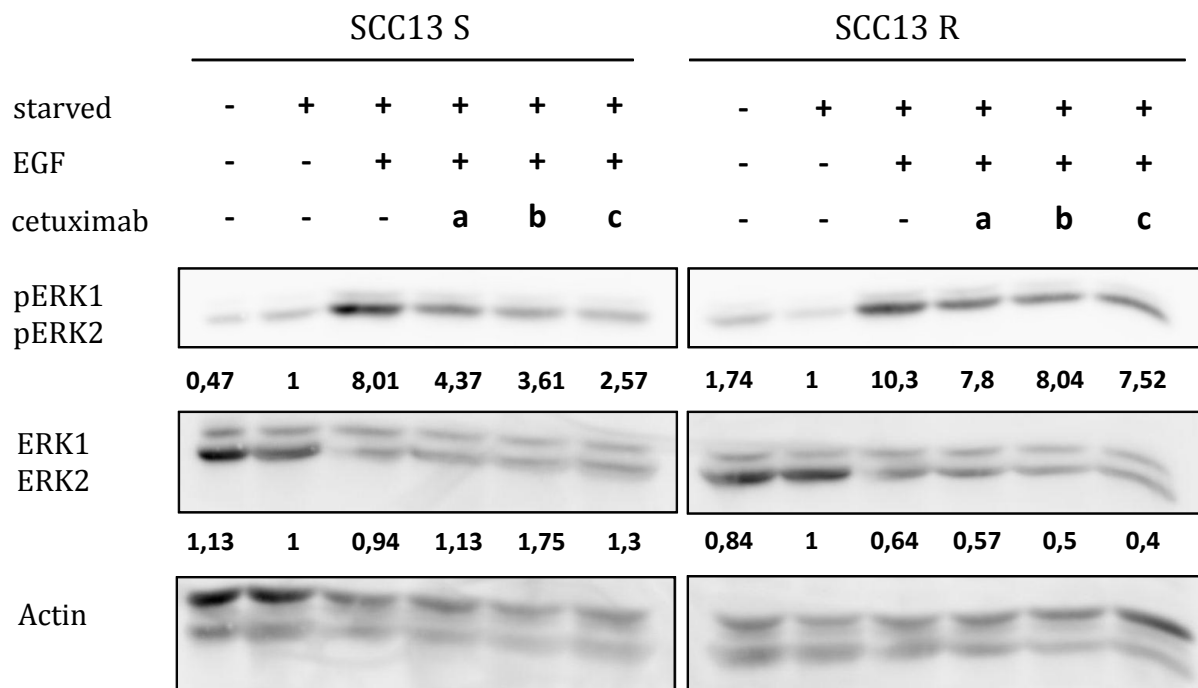
Figure 12: EGFR signaling profile of cetuximab-resistant cells. Sensitive as well as resistant cells of the cell line SCC13 were cultured under starvation conditions and exposed to different concentrations of cetuximab (a = 10 µg/ml, b = 100 µg/ml, c = 1000 µg/ml) for 1 h followed by 20 min of EGF stimulation. As controls, cells were cultured under normal conditions w/o treatment, in starvation medium w/o treatment as well as under starvation conditions with stimulation of EGF (w/o pre-treatment of cetuximab). After harvesting, cells were lysed and processed for immunoblotting using antibodies directed against pERK1/2 and ERK1/2. Actin served as a loading control. Quantification of Western blot analysis was done by ImageJ 1.46 (NIH), and the numbers are provided at the bottom of each Western blot, respectively.

3.2.3 Growth of cetuximab-sensitive and –resistant (HN)SCC cell lines as xenografts in nude mice

Tumor cell lines which are introduced as xenografts into nude mice can potentially model complex interactions between the tumor and its host. One concern of culturing cells *in vitro* is the adaption of tumor cells to the culture environment and the development of genetic and phenotypic differences from the original tumor. Another major concern associated with acquired resistance against a drug, is that different cellular processes such as proliferation and survival might be altered during this selective process. To address this question, the growth of the individual cell lines applied as xenografts in nude mice was examined. Furthermore, I analyzed, whether there was a difference in the tumorigenic potential of cetuximab-resistant and -sensitive cells. The athymic nude mouse is the most commonly used immunodeficient mouse model to study head and neck cancer, which carries a homozygous nu mutation on mouse chromosome 11 leading to thymic dysgenesis (Rygaard and Poulsen, 1969). The primary immune defect of these mice is a T-cell deficiency to prevent graft rejection. However, the athymic nude mouse, on the other hand, is not completely immunodeficient, by having B cells, natural killer (NK) cells as well as macrophages. Based on the previous results, I used a mouse xenograft model to determine how the resistant cells which were developed *in vitro* would grow *in vivo* in contrast to the parental, untreated cells. The experiment was performed by injecting 1×10^6 cetuximab-sensitive as well as cetuximab-resistant cells into the dorsal flank area of athymic nude mice. Figure 13 shows the tumors on the dorsal area of athymic nude mice. The picture was taken from a preliminary experiment, in which the correct cell concentration, needed to induce tumors in the mice, was examined. As shown, all three (HN)SCC cell lines (HNSCC11, SCC13 and HNSCC22) induced tumors in the mice.

Figure 13: Tumor formation of (HN)SCC cell lines HNSCC11, SCC13 and HNSCC22 in athymic nude mice.

For the main experiment, four mice per cell line (SCC13 S, SCC13 R, HNSCC22 S and HNSCC22 R) were injected with the cells. The tumor size was measured once to twice a week, and calculated using the formula stated in Materials and Methods. The *in vivo* results indicated that for both cell lines the cetuximab-sensitive cells formed slightly bigger tumors in nude mice compared to the resistant cells during the first three weeks of the experiment. Furthermore, the resistant cells seemed to grow slightly slower in xenografts (Figure 14). These results suggest that all cell lines retained their proliferative potential *in vivo*, although there were no significant differences in the size of orthotopic tumors derived from sensitive and resistant cell lines.
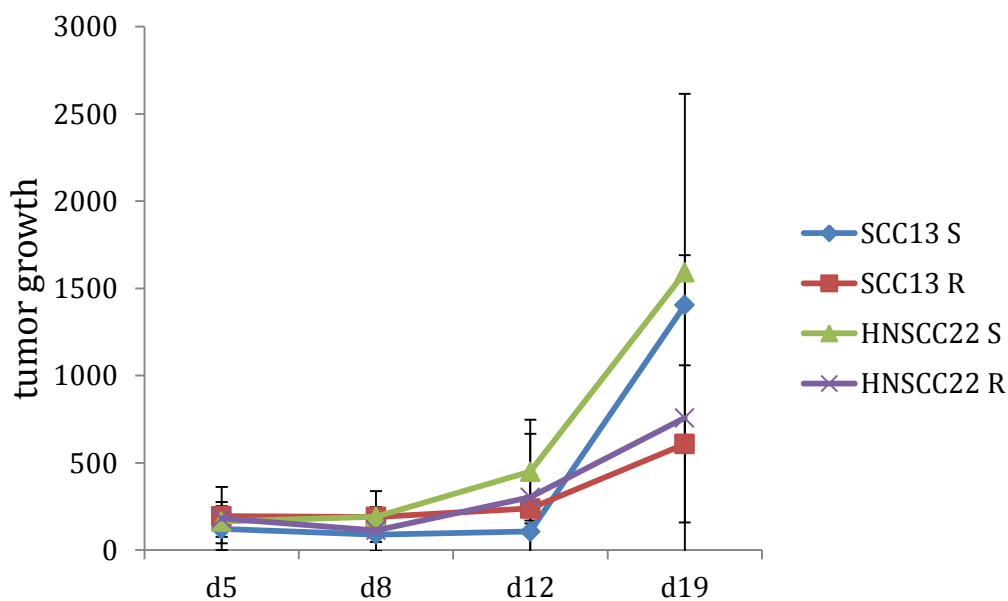
Figure 14: Growth of cetuximab-sensitive and -resistant (HN)SCC cell lines (SCC13 S, SCC13 R, HNSCC22 S and HNSCC22 R) as xenografts in nude mice. $1*10^6$ cells were injected subcutaneous into the dorsal flank area of nude mice. The tumor size was measured 1-2 times a week. Shown is the average tumor size of the tumors in four mice per cell line ± SD.

3.2.4 Gene expression analysis of the EGFR and different chromatin factors

In order to analyze the gene expression of the EGFR and to investigate whether epigenetic mechanisms might play a role in the acquired resistance against cetuximab I performed a real-time PCR analysis. I analyzed the gene expression of various chromatin factors in the (HN)SCC cell lines SCC13 S/R and HNSCC22 S/R. The real-time PCR analysis (Figure 15) revealed that the two parental cell lines express major chromatin regulators such as *EZH2* and *JMJD3* (H3K27me3) or *DNMT1* (DNA methylation) at different levels. However, these levels stay equal upon acquiring resistance towards cetuximab. On the contrary, EGFR levels were significantly induced in the resistant cell lines (SCC13 p=0,02; HNSCC22 p=0,005).
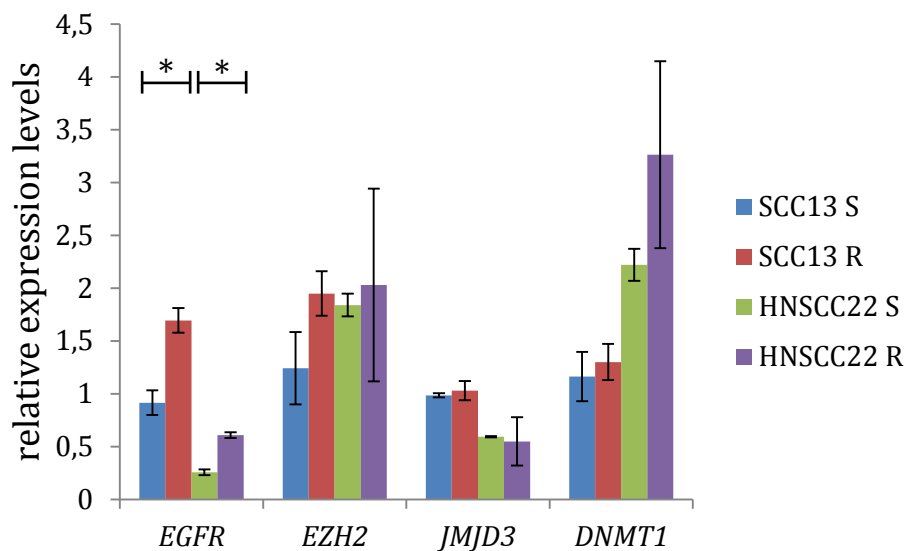
Figure 15: Relative expression levels of *EGFR, EZH2, JMJD3* and *DNMT1* in resistant and sensitive SCC13 and HNSCC22 cell lines. Data represent mean of technical replicates ± SD. * indicates significance (* p≤0,05).

In order to understand to what extent acquired cetuximab resistance changes the cellular identity, I performed transcriptional profiling of both sensitive and resistant (HN)SCC cell lines, comparing the "transcriptomes" by RNA Sequencing. Comparing gene expression in cetuximab-sensitive HNSCC cells and their resistant counterparts revealed the full extent of the impact of acquired cetuximab resistance and uncovered changes in transcriptional programs, which could contribute to the pathogenicity of HNSCC in patients.

3.3 Next generation sequencing - Transcriptomic and epigenomic comparison of sensitive and resistant cells

Next generation sequencing was performed to provide a detailed insight into the (epi-) mutations causing or appearing in acquired cetuximab resistance. RNA- and WGB-sequencing libraries of cetuximab- sensitive as well as -resistant cell lines were generated in order to determine the differences in gene expression and DNA methylation. These samples were sequenced afterwards. However, it was necessary to examine the quality of the samples prior to loading the samples on a flow cell. Figure 16 shows that the samples met all quality criteria necessary for loading on a flow cell, thus indicating that the generation of the libraries was successfully performed.

a
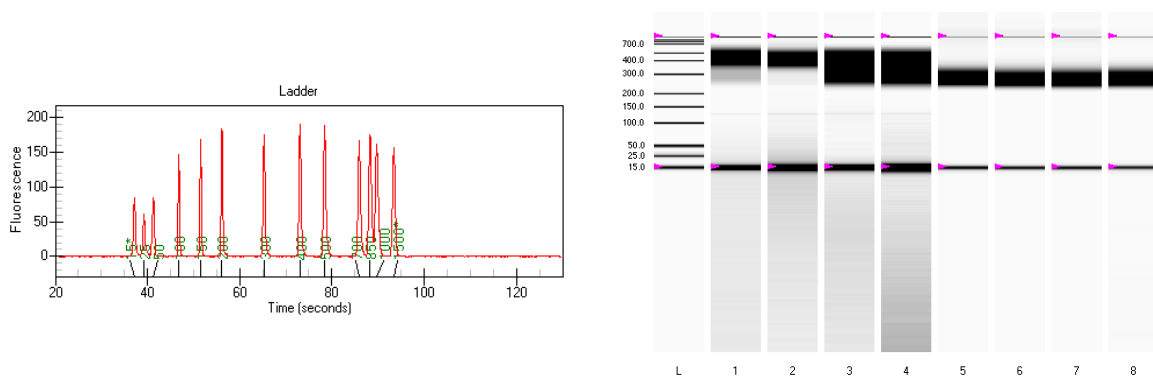
b
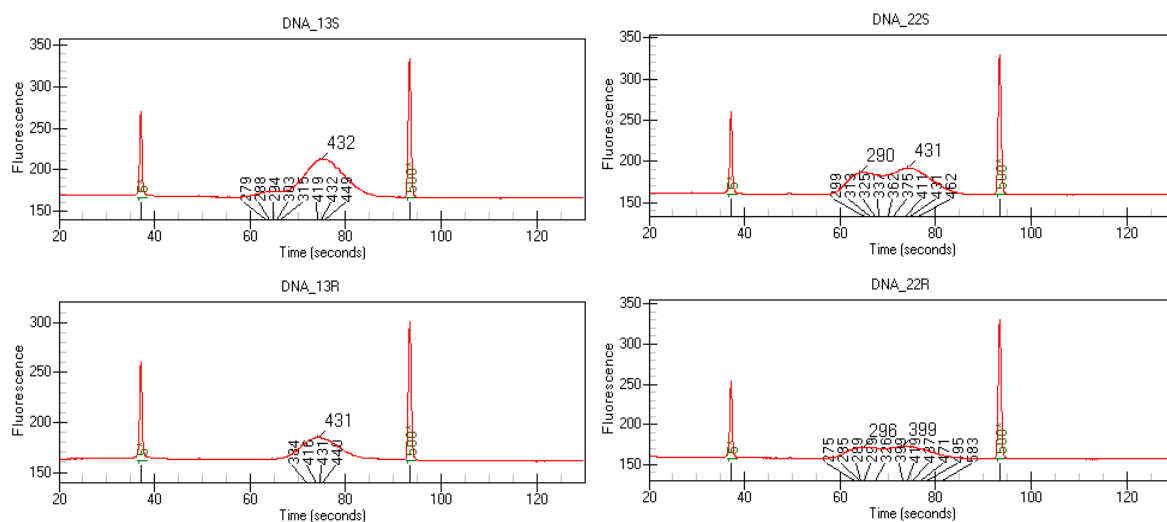
c
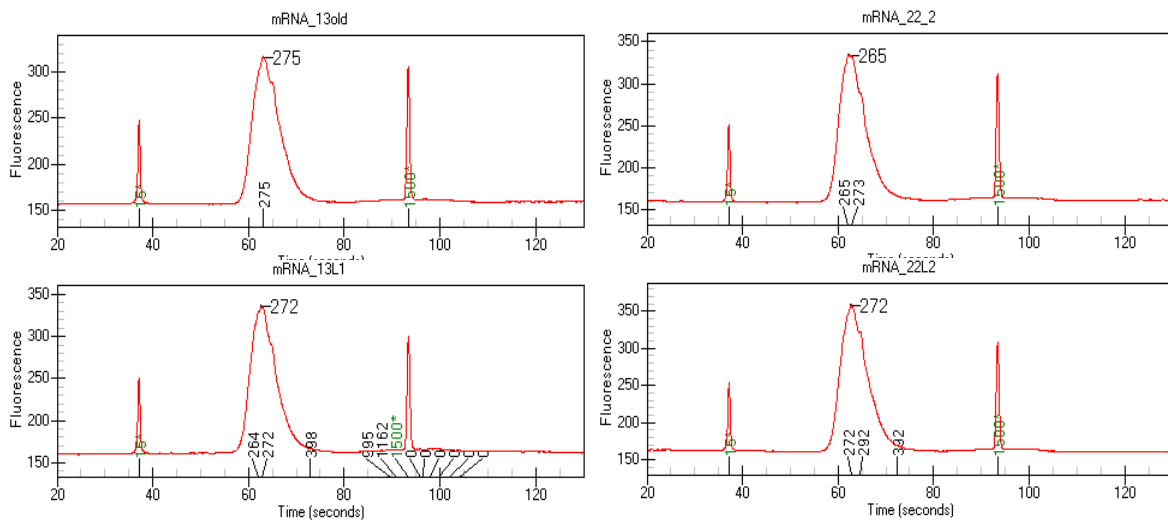
Figure 16: Preparation of libraries for NGS: (a) Ladder; (b) WGB-libraries and (c) mRNA-libraries ready for Illumina-sequencing. All libraries met the quality criteria necessary for loading on a flow cell.

3.3.1 Whole-genome bisulfite sequencing

The result of the WGBS (Table 1) indicated that there were no global differences in DNA methylation between the sensitive and resistant cells. This result suggests that loss or gain of genome wide DNA methylation is not necessary for cetuximab resistance.

Table 1: Genome wide DNA methylation of cetuximab-sensitive and –resistant cell lines

Cell line	Genome wide DNA methylation (WGBS)
SCC13S	56,70%
SCC13R	57,90%
HNSCC22S	61,50%
HNSCC22R	60,10%

3.3.2 RNA Sequencing

3.3.2.1 Verification of gene expression of top up/down-regulated genes via qPCR

The result of the RNA Sequencing analysis revealed the expression of 23284 genes for the parental (SCC13 S and HNSCC22 S) and the resistant (HN)SCC cell lines (SCC13 R and HNSCC22 R). The genes in the resistant cell lines having either more than +1 (top up-regulated) or less than -1 (top down-regulated) log2 fold change were selected from the gene expression list. Afterwards, they were imported into the VENNY software[5] to construct a VENNY diagram, which allowed the comparison of the genes and indicated which ones are overlapping in the specific lists. Figure 17 shows the interference of 129 genes, up-regulated (left) in both cetuximab-resistant cell lines, and 161 genes, which were down-regulated (right) in both cetuximab-resistant cell lines. This result suggests that identical genes can be found in cell lines from different origins in the body which are either up- or down-regulated after acquiring resistance to cetuximab.
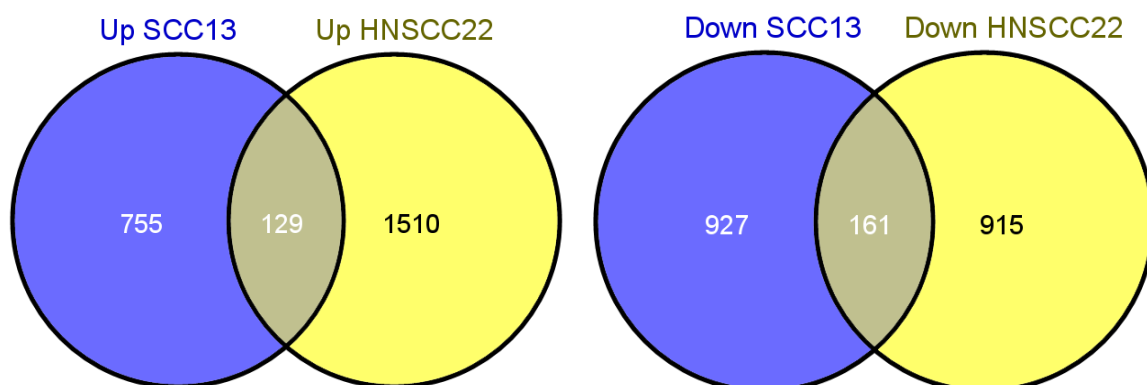
Figure 17: VENNY diagram showing the overlap of top up- (left) and top down-regulated (right) genes in the cetuximab-resistant cell lines SCC13 and HNSCC22.

The RNA Sequencing result was verified by performing real-time PCR analysis. Therefore, the top up- and down-regulated genes were selected and compared. For specific genes (*KLRK1, DUSP6, TOX2, CBX2, S100A7, PI3, JMJD7-PLA2G4B, ZNF177 and IFI27*), having functions of interest in cancer development or signaling cascades[6], primers were designed. The expression of the genes in the cetuximab-sensitive and -resistant cell lines as well as the log2fold change is shown in Table 2. Figure 18 displays

---

[5] http://bioinfogp.cnb.csic.es/tools/venny/index.html
[6] http://www.genecards.org/

the result of the real-time PCR analysis. The results were comparable to the ones of the RNA Sequencing analysis with the exception of the genes *JMJD7-PLA2G4B* and *ZNF177,* in which the expression was expected to be higher in the cetuximab-sensitive cell line SCC13. With regard to the cell line HNSCC22, the tendency of the gene expression for all genes, with the exception of *KLRK1* and *ZNF177,* in which the expression was expected to be higher in the sensitive cell line, was also comparable with the RNA Sequencing result.

Table 2: RNA Sequencing result of the genes *KLRK1, DUSP6, TOX2, CBX2, S100A7, PI3, JMJD7-PLA2G4B, ZNF177 and IFI27*. The table shows the gene expression of the cell lines SCC13 S/R and HNSCC22 S/R as well as the log2 fold change.

Gene	mRNA SCC13 S	mRNA SCC13 R	mRNA SCC13 log2 fold change	mRNA HNSCC22 S	mRNA HNSCC22 R	mRNA HNSCC22 log2 fold change
KLRK1	0,01	0,06	3,52	0,04	0,16	1,84
DUSP6	0,24	2,14	3,16	0,10	0,45	2,17
TOX2	0,49	1,24	1,34	0,03	0,43	4,03
CBX2	0,03	0,25	2,86	0,06	0,26	2,01
S100A7	15,93	0,93	-4,10	0,98	0,13	-2,88
PI3	29,11	2,36	-3,62	1,15	0,09	-3,68
JMJD7-PLA2G4B	0,52	$1,4*10^{-5}$	-15,17	$2,5*10^{-5}$	0,10	12,04
ZNF177	0,07	$9,8*10^{-5}$	-9,46	$5,5*10^{-6}$	0,09	14,03
IFI27	1,28	0,10	-3,71	0,26	0,07	-1,86
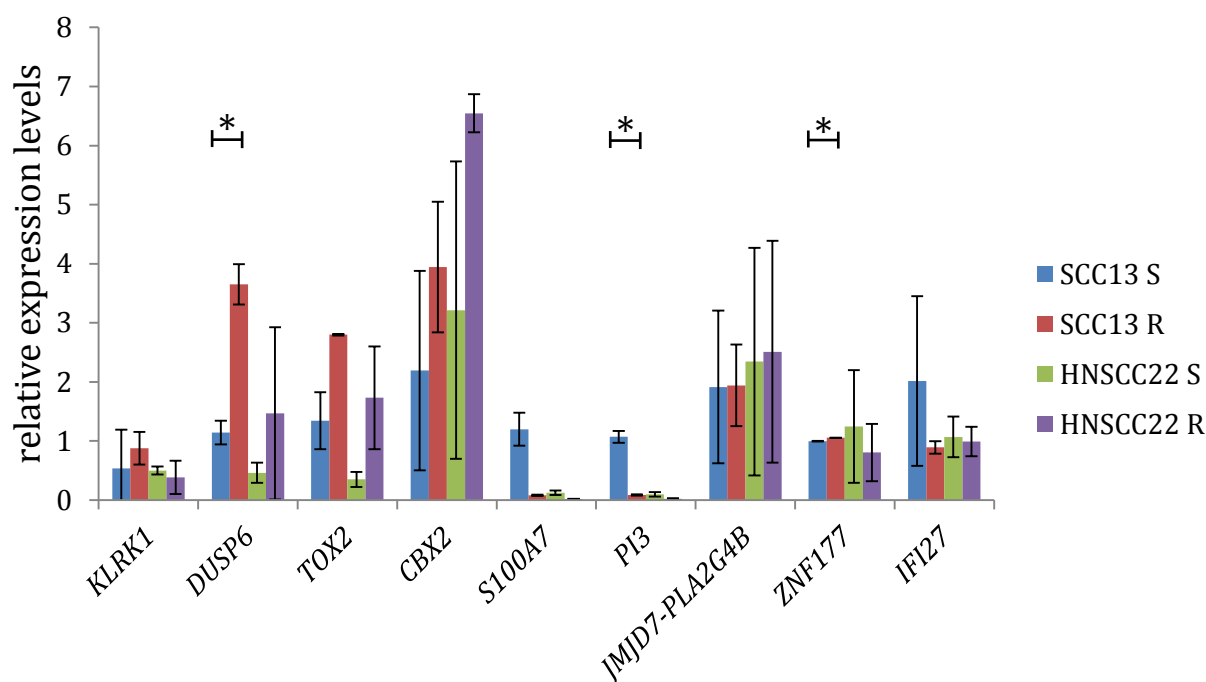
Figure 18: Relative expression levels of *KLRK1, DUSP6, TOX2, CBX2, S100A7, PI3, JMJD7-PLA2G4B, ZNF177* and *IFI27* in cetuximab-sensitive and -resistant cell lines (SCC13 S/R, HNSCC22 S/R). Data represent mean of technical replicates ± SD. * indicates significance (* p≤0,05).

3.3.2.2 Gene expression of human epigenetic chromatin remodeling factors

To investigate whether there was any difference in the gene expression of human epigenetic chromatin remodeling factors between cetuximab-sensitive and –resistant cells, the RNA Sequencing results were analyzed. Indeed, different genes were up-regulated as well as one gene down-regulated in the resistant cell lines SCC13 R and HNSCC22 R (Table 3). In the cell line SCC13 R the gene *BRDT* was up-regulated and *HDAC9* down-regulated. *BRDT* is a gene belonging to the bromodomain proteins that are able to recognize acetylated lysine residues such as those on the N-terminal tails of histones. *HDAC9* is a histone deacetylase and catalyzes the removal of acetyl groups from lysine residues in histones and non-histone proteins. This action results in transcriptional repression. In the cell line HNSCC22 R different epigenetic chromatin remodeling factors were up-regulated. *BMI1* as well as *PCGF5* are both belonging to the Polycomb group genes and known to be involved in epigenetic silencing of genes. Furthermore, it could be shown that *CHD1* and *CHD5* (chromodomain-helicase-DNA-binding protein) were both up-regulated in this cell line. The CHD family of proteins is characterized by the presence of chromo domains and SNF2-related helicase/ATPase domains. They alter the gene expression possibly by modification of the chromatin

structure (Kelley et al., 1999). *CBX3* is a chromodomain/Heterochromatin Protein 1 (HP1) homolog and binds histone H3 tails methylated at Lys-9 sites and is a component of heterochromatin. The last gene found to be overexpressed in HNSCC22 R is *MTA2*. This gene is a nucleosome-remodeling and histone deacetylase (NuRD) complex component. The result shows that several epigenetic chromatin remodeling factors are deregulated in the resistant cell lines compared to the sensitive ones.

Table 3: RNA Sequencing result of the genes *BRDT, HDAC9, BMI1, PCGF5, CBX3, CDH1, CDH5 and MTA2.* The table shows the gene expression of the cell lines SCC13 S/R and HNSCC22 S/R as well as the log2 fold change.

Gene	mRNA SCC13 S	mRNA SCC13 R	mRNA SCC13 log2 fold change
BRDT	0,01	0,04	1,46
HDAC9	1,18	0,55	-1,11

Gene	mRNA HNSCC22 S	mRNA HNSCC22 R	mRNA HNSCC22 log2 fold change
BMI1 (PCGF4)	0,06	0,18	1,53
PCGF5	0,20	0,96	2,23
CBX3	2,41	4,91	1,03
CHD1	0,47	0,95	1,03
CHD5	0,01	0,02	1,35
MTA2	1,64	3,38	1,04

3.3.2.3 Gene expression of *VEGFA*, *VEGFC*, *FLT1* and *EGFR* in cetuximab-sensitive and –resistant (HN)SCC cell lines

In addition to the top up- and down-regulated genes, four further genes of special interest for our study comprise *EGFR* and *VEGFA*, *VEGFC* and *FLT1* (Table 4), knowing that VEGF signaling synergizes with EGFR in tumor cells to promote cancer development in epithelial cells (Lichtenberger et al., 2010). *EGFR*, *VEGFA* and *VEGFC* were up-regulated and *FLT1* down-regulated in the cetuximab-resistant cell line HNSCC22 R. *EGFR*, *VEGFA* and *FLT1* were up-regulated in the cell line SCC13 R. These results suggest that the VEGF pathway is deregulated in cetuximab-resistant cell lines.

Table 4: RNA Sequencing result of the genes *EGFR*, *VEGFA*, *VEGFC* and *FLT1*. The table shows the gene expression of the cell lines SCC13 S/R and HNSCC22 S/R as well as the log2 fold change.

Gene	mRNA SCC13 S	mRNA SCC13 R	mRNA SCC13 log2 fold change	mRNA HNSCC22 S	mRNA HNSCC22 R	mRNA HNSCC22 log2 fold change
EGFR	17,99	20,27	0,17	2,95	9,26	1,65
VEGFA	2,17	4,49	1,05	0,92	6,22	2,76
VEGFC				0,49	1,17	1,25
FLT1	0,02	0,06	1,88	0,19	0,16	-0,22

3.3.2.4 Bioinformatic analysis of RNA Sequencing data

The data of the RNA Sequencing analysis was further evaluated. In the biological network, 14 of the top up-regulated genes were found to interact with each other. Furthermore, the genes were very heterogeneous in the network due to diverse regulation. Figure 19 shows the 103 most strongly induced genes in the cetuximab-resistant cell lines SCC13 R and HNSCC22 R which may also serve as biomarkers. Among these genes, *VEGFA* as well as *VIM* were detected. *VIM* is known to play a role in the process of epithelial to mesenchymal transition (EMT) in HNSCC (Keysar et al., 2013; Smith et al., 2013; Squarize et al., 2013). We performed a functional clustering analysis of the deregulated genes in cetuximab-resistant cell lines and could confirm that most of these genes were involved in pathways such as "the positive regulation of calcium ion transport" (Figure 20). In summary, the results of the bioinformatic analysis show the involvement of different pathways in the acquired resistance to cetuximab and a very heterogeneous gene regulation. Furthermore, we could identify several biomarkers which are interesting targets for cancer therapy.
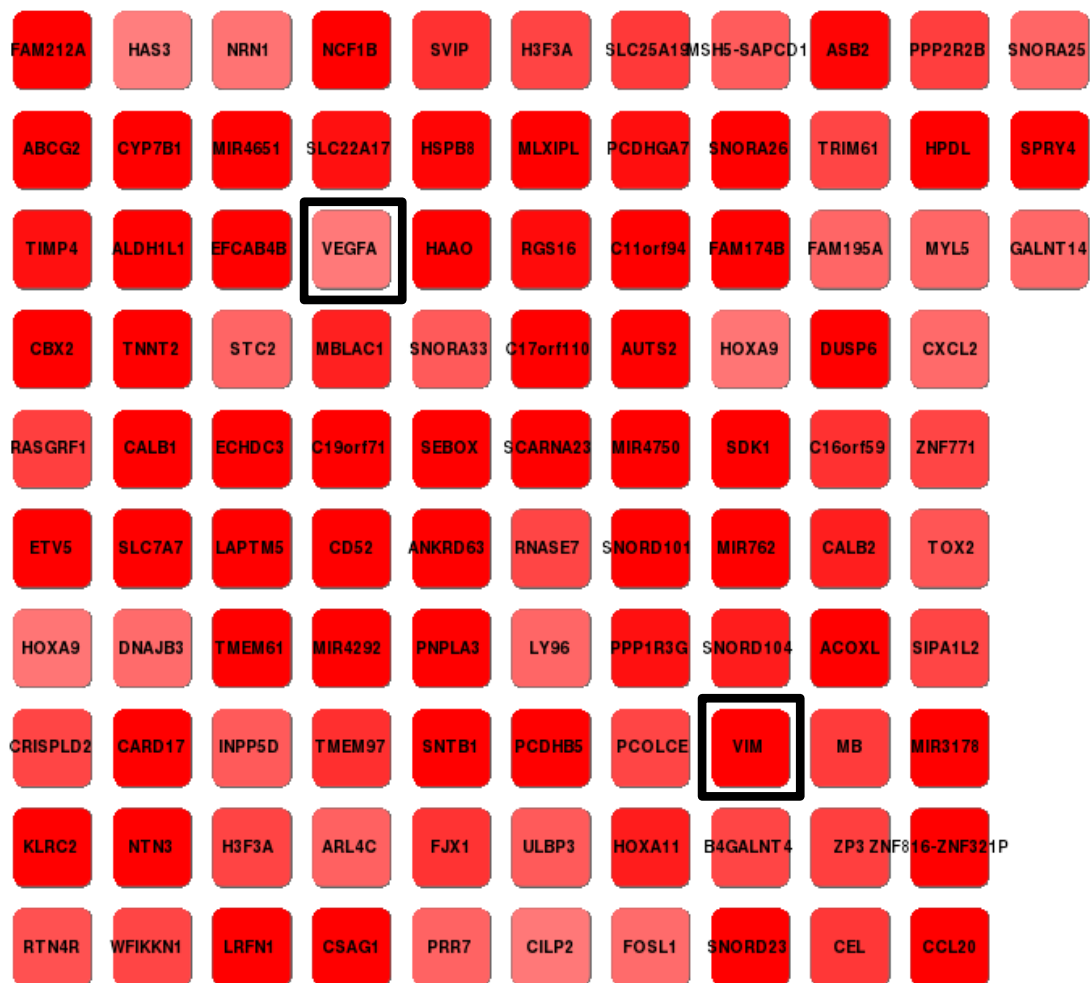
Figure 19: Most strongly induced genes in cetuximab-resistant cell lines.
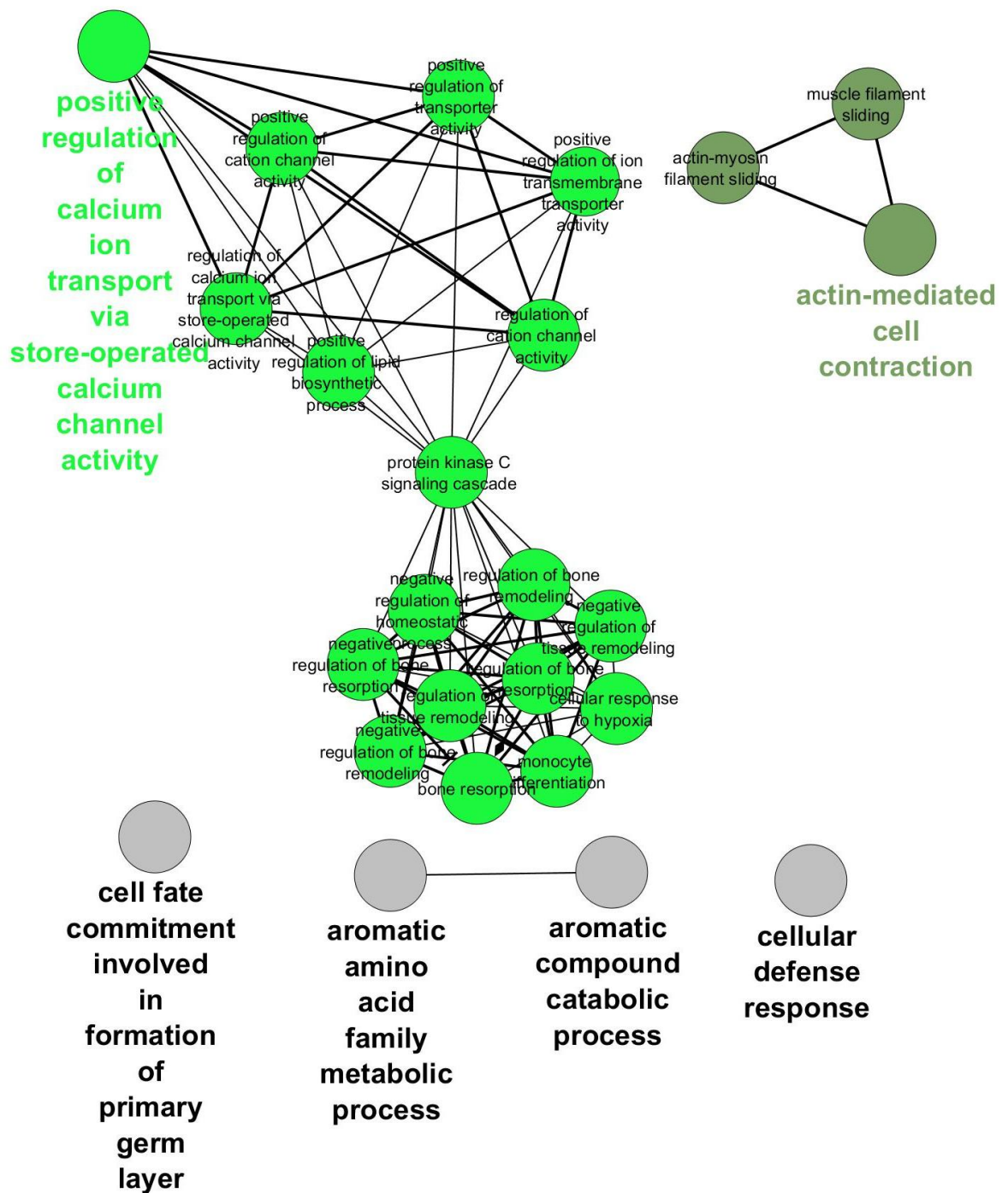
Figure 20: Functional clustering of genes deregulated in cetuximab-resistant cell lines.

3.4 Influence of VEGF on cetuximab-sensitivity in (HN)SCC cell lines

Since *VEGFA* was up-regulated in both resistant cell lines compared to the sensitive ones, I performed an MTT assay to analyze the effect of VEGF on the proliferative potential of cetuximab-sensitive cells, while being exposed to cetuximab. This experiment should reveal whether reduced cetuximab-sensitivity in cetuximab-resistant

cell lines resulted from increased *VEGF* expression. Thus, I expected that the cetuximab-sensitive cell lines, being exposed to VEGF, would lose cetuximab-sensitivity and show increased growth compared to the sensitive cells being exposed to cetuximab only. To test this hypothesis, the cells were treated with different concentrations of cetuximab (5 µg/ml, 10 µg/ml, 25 µg/ml and 50µg/ml) for 48 h and cultured alone or in the presence of EGF or VEGF. Furthermore, cells were exposed to VEGF (30 ng/ml) w/o cetuximab treatment. Figure 21 shows survival curves of the SCC cell line SCC13 S and the HNSCC cell line HNSCC22 S, which were treated with VEGF only (a), cetuximab only or in the presence of EGF or VEGF (b and c) for 48 hours. The exposure to VEGF resulted in increased cell viability in the cell line SCC13 S, whereas a decrease in cell viability was seen in the cell line HNSCC22 S. Furthermore, increasing concentrations of cetuximab resulted in decreased cell viability in both cell lines. Surprisingly, it turned out that the combination of EGF or VEGF with cetuximab strengthened the inhibitory effect of cetuximab in both cell lines. The result of the experiment shows that although VEGF led to a slight increase in proliferation in the cell line SCC13 S and to a slight decrease in cell viability in the cell line HNSCC22 S, in combination with cetuximab it increases the inhibitory effect of the drug.

a

b

c
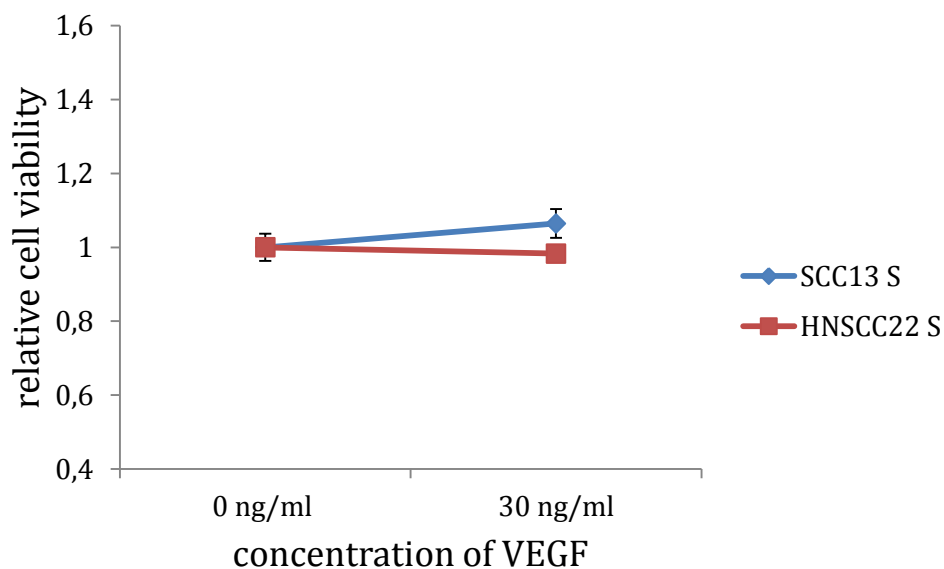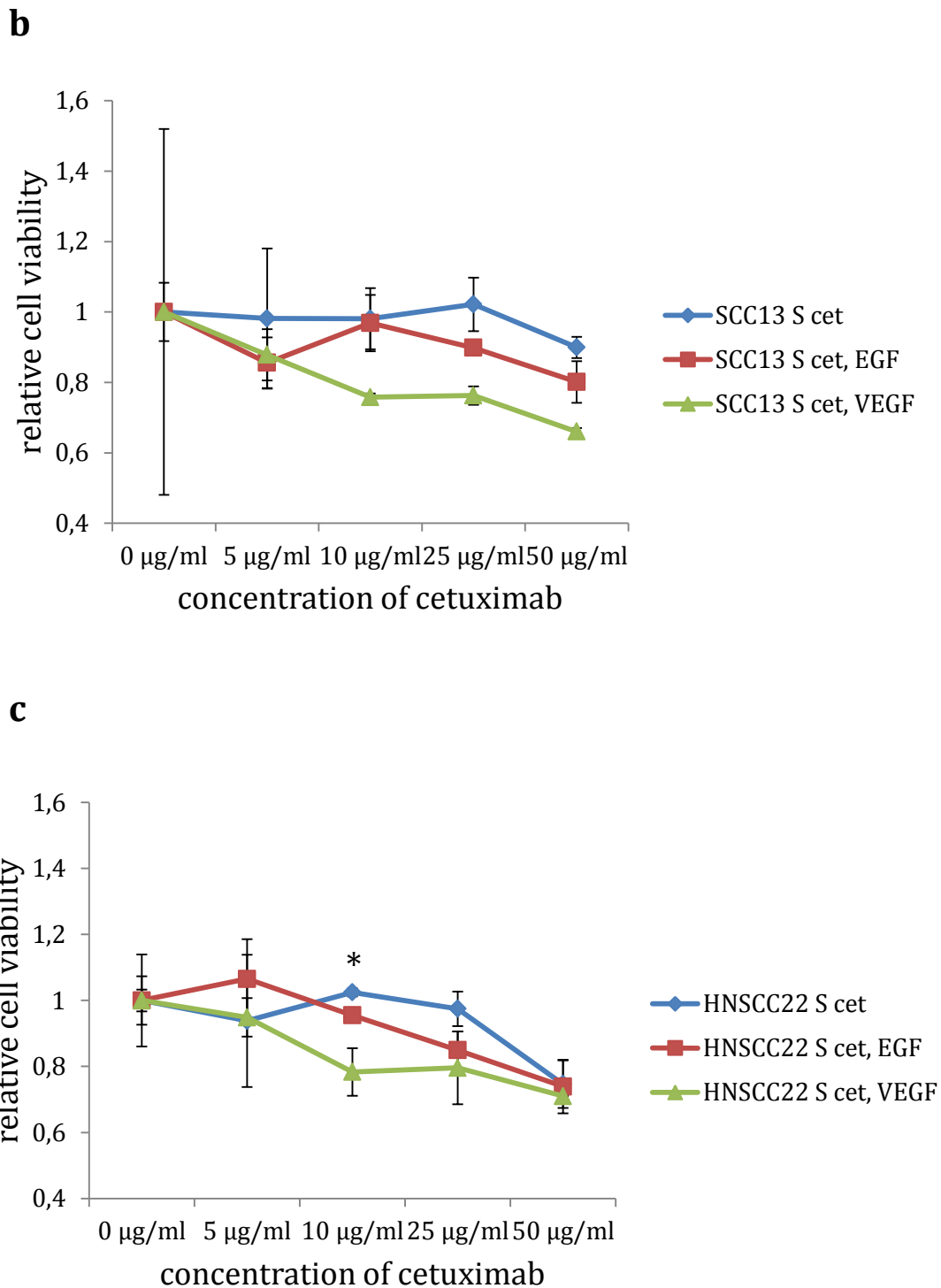
Figure 21: Survival curves of the (HN)SCC cell lines SCC13 S (a, b) and the HNSCC22 S (a, c). Cells were exposed to VEGF (a) or to cetuximab alone or in the presence of EGF or VEGF (b, c) for 48 hours. The result was confirmed in another experiment. Data represent mean of biological duplicates ± SD. * indicates significance (p≤0,05).

4 Discussion

4.1 Characterization of cetuximab-sensitive and –resistant (HN)SCC cell lines

Molecular inhibition of EGFR signaling, as a promising target of cancer therapy, is under active investigation. However, acquired resistance to EGFR inhibitors can be found more and more in preclinical model systems as well as in cancer patients who initially seem to respond well to the treatment (Engelman and Jänne, 2008; Kwak et al., 2005; Pao et al., 2005; Viloria-petit et al., 2001; Yamasaki et al., 2007). Thus, there is an urgent need to better understand the underlying mechanisms of acquired cetuximab resistance as it was shown that EGFR inhibitor-resistant tumors may also become cross-resistant to other drug or treatment alternatives with different mechanisms of action (Benavente et al., 2009; Camp et al., 2005).

One head and neck squamous cell carcinoma (HNSCC22) and one squamous cell carcinoma (SCC13) cell line, respectively, resistant to cetuximab, were generated in this Master′s thesis, to analyze mechanisms of acquired resistance to the EGFR inhibition. The applicability of the initially EGFR inhibitor-sensitive (HN)SCC cell lines for the process of generating resistant cell lines was confirmed since the cells revealed strong phosphorylation of ERK1/2, which lies downstream of the EGFR signaling cascade, after stimulation with EGF as well as decreased phosphorylation after inhibition with BIBW 2992 and cetuximab. Hence, the EGFR responded normally and was not mutated. The gene expression analysis of different epigenetic markers as well as known oncogenes revealed that the relative gene expression of nearly all analyzed genes was higher in the SCC cell line 13 in contrast to the HNSCC cell lines 11 and 22, which showed same expression levels of all analyzed genes. The cell line SCC13 was isolated from facial epidermis in contrast to the cell lines HNSCC11 and HNSCC22, which stem from the head and neck. Hence, different gene expression profiles probably resulted from varying origins of the used cells. Next, I analyzed in which way cetuximab led to the decreased cell count *in vitro*, which was observed after exposure to the drug, as it is known that cetuximab can lead to apoptosis as well as decreased proliferation (Zimmermann et al., 2006). The analysis of the apoptotic potential of cetuximab revealed a significant increase in early-stage apoptosis after 48 h of cetuximab exposure in the cell line SCC13, whereas no significant increase could be observed in early-stage apoptosis after 24 h as well as in late-stage apoptosis. With regard to the cell line HNSCC22, cetuximab treatment did not result in a significant increase in early- or late stage apoptosis after 24

h and 48 h of treatment. This result was confirmed by the result of the TUNEL staining. These findings underscore that the decrease in cell count after cetuximab exposure might result from a decrease in cell proliferation rather than from apoptosis. To test this hypothesis, a proliferation analysis was performed. The result showed significantly decreased proliferation in the cell line SCC13, after exposure to cetuximab for 48 h over a growth period of 16 h, suggesting that one reason for the cetuximab-induced decrease in cell count is decreased proliferation after exposure to the drug. Building on these results it would be interesting to further investigate the molecular properties of the cell lines. It will be particular interesting whether the decrease in proliferation is stronger if the duration of exposure to the inhibitor is extended. Building on our preliminary results regarding the inhibition of ERK1/2, I will also focus my attention on AKT signaling, as it is known that it lies downstream of EGFR activation and is implicated in the survival of cells (Sibilia et al., 2000). In addition, the activation of alternative pathways (IGF-1R, mTOR, VEGFR and Herb-B2) as well as the constitutive activation of downstream signaling pathways (e.g. PI3K/Akt, MAPK, p27, cyclin D1, PTEN mutations) are known to be possible mechanisms of resistance to EGFR inhibitors (Morgillo et al., 2007). The analysis could be done by immunoblot analysis as well as by measuring of cell proliferation (via ERK activation) and survival or rather apoptosis (AKT activation). In particular, with respect to resistance mechanisms, the results would indicate, whether resistance to cetuximab is mainly achieved by increased cellular proliferation, survival or both. Starting with the IC$_{50}$% value of cetuximab and doubling the concentration after every 2nd cell passage, I succeeded in generating resistant cells after 7 months (corresponding 14 passages), which was confirmed by a MTT assay (Figure 11) as well as on the protein level (Figure 12). After the generation of resistant cell lines, I isolated RNA, protein as well as DNA for molecular analyses. Additionally, to show that the cells were still able to grow *in vivo*, I analyzed the growth of cetuximab-sensitive and -resistant cell lines as xenografts in athymic nude mice. The results showed that our cells survived and did not lose the ability to grow *in vivo* because of an alteration in cellular processes such as proliferation and survival as it is a concern during this selective process. Instead of that, I could show that cells which are sensitive as well as resistant to cetuximab could form xenografts in athymic nude mice. However, there was no significant difference in the size of the tumors, guessing that the resistance against cetuximab did not have an influence on the proliferative potential of the cells. Based on these results it would be interesting to perform an *in vivo* treatment with cetuximab

after introducing cetuximab-sensitive and –resistant cell lines as xenografts into nude mice and analyze the cell populations at the end of the treatment as it was performed by Keysar et al. (2013). This would give information whether the population has changed to a more mesenchymal phenotype and would favor EMT which is known to be a process in the acquired resistance (Morgillo et al., 2007).

4.2 Next generation sequencing of cetuximab-sensitive and -resistant (HN)SCC cell lines

Not only the genome but also the epigenome must be examined in detail in order to better understand the process of carcinogenesis (Esteller, 2006). Thus, I performed a real-time PCR analysis to analyze the gene expression of the *EGFR* as well as of the epigenetic markers *EZH2*, *JMJD3* and *DNMT1*, in the cetuximab-sensitive as well as in the -resistant cell lines. *EZH2*, or enhancer of zeste homolog 2, is a histone-lysine N-methyltransferase, leading to transcriptional repression of the affected target gene, after methylation of H3K9 or H3K27. *JMJD3* is a histone H3 Lys 27 demethylase and regulates the gene expression by impacting transcriptional elongation (Chen et al., 2012). *DNMT1*, also known as DNA (cytosine-5)-methyltransferase 1, methylates CpG residues, preferentially hemimethylated DNA. It is associated with DNA replication sites in S phase maintaining the methylation pattern in the newly synthesized strand, essential for epigenetic inheritance. The *EGFR* levels were induced significantly in both resistant cell lines (SCC13 R and HNSCC22 R), most likely as a straight compensatory mechanism. In contrast to that, the few epigenetic factors which I analyzed so far were not differentially expressed between cetuximab-sensitive and -resistant cells. However, this result does not preclude the possibility that the epigenomic patterns of the marks regulated by these factors are altered in the resistant cells. In order to understand to what extent acquired cetuximab resistance changes the cellular identity, we performed next generation sequencing for DNA sequences enriched for these marks. The NGS-data were evaluated by focusing on the question whether conserved (epi-)genetic mutations, involved in the acquired resistance against cetuximab, could be detected. The result of the WGBS (Table 1) revealed no global differences in DNA methylation between the sensitive and resistant cells, meaning that loss or gain of genome wide DNA methylation is not necessary for cetuximab resistance. Nevertheless, I examined whether there were any differences in candidate genes. Therefore, promoter sequences were compared on the basis of the 50 base pair reads and it was analyzed whether there were any

differences in the gene expression because of differences in the DNA methylation. I chose five candidate genes and compared the DNA methylation of the promoter region in the resistant compared to the sensitive cell lines. However, no difference in the DNA methylation could be observed. Nevertheless, it would be interesting to analyze more genes. The results of the RNA Sequencing showed that of all analyzed genes 129 identical genes could be found which were up-regulated in both resistant cell lines (SCC13 R and HNSCC22 R). Furthermore, 161 identical genes were found to be down-regulated in both resistant cell lines. The gene expression of the top up- and down-regulated genes was verified via real-time PCR analysis. However, since we are interested in epigenetic mechanisms, regulating acquired resistance, I analyzed the gene expression of known human epigenetic chromatin remodeling factors. Epigenetic mechanisms are powerful regulators of transcription and often deregulated in cancer (Berdasco and Esteller, 2010). In our group, we have found that Dnmt1 levels are severely reduced in EGFR-deficient cells (unpublished), suggesting that DNA-methylation might be a pathway through which EGFR-signaling regulates parts of the epigenome. Based on the methylation status of a gene, tumor suppressor genes can be uncovered, providing new information about therapy strategies (Esteller, 2006). Research results show that the methylation is a very early event in carcinogenesis and it does not only lead to the inactivation of the corresponding genes, but also favors additional genetic alterations in the cell (Esteller, 2006; Herranz and Esteller, 2006). Thus, in several carcinomas the methylation status is used as a prognostic marker (Verma et al., 2006). With respect to HNSCC a hypermethylation of p16 (INK4a) could be identified in precursors and correlated with the tumor stage (Weber et al., 2003). However, as shown by the result of the real-time PCR analysis, the WGBS as well by examining our RNA Sequencing results, I could not find a deregulation of Dnmt1 in the resistant cell lines compared to the sensitive ones. Therefore, I concentrated on other chromatin remodelers. Although, I did not find identical genes which were up- or down-regulated in both resistant cell lines, I could show that different chromatin remodelers were elevated or down-regulated in either of the resistant cell lines SCC13 R and HNSCC22 R (Chapter 3.3.2.2.), thus leading to the assumption that chromatin remodeling might play an important role with respect to acquired resistance to cetuximab. A total of 103 genes were revealed as potential biomarkers by bioinformatics analysis of the RNA Sequencing data of the top up-regulated genes in both resistant cell lines. One gene of special interest is *VIM*, which is known to play an important role in the

process of EMT in HNSCC (Keysar et al., 2013; Smith et al., 2013; Squarize et al., 2013). The process by which a tumor cell with epithelial characteristics transitions to a tumor cell with mesenchymal characteristics (Smith et al., 2013) is important in the initiation of metastasis for cancer progression. These results suggest that the cetuximab-resistant tumor cells have undergone a transition to a more mesenchymal cell type. A functional clustering of the deregulated genes in cetuximab-resistant cells showed that several pathways were involved and that the gene regulation was thus very heterogeneous. Based on the previous results, it would be interesting to investigate whether interference with major epigenetic pathways may preclude the acquisition of cetuximab-resistance in HNSCC, or if in later stages, it would lead to a reversion to the sensitive state in resistant cells. On the other hand, it would be questionable, if cetuximab-resistant cells could be generated after interfering with epigenetic regulators. For this approach shRNA mediated knock-down of deregulated epigenetic chromatin remodelers could be performed and analyzed whether this would restore cetuximab sensitivity. To clarify whether these epigenetic pathways actively establish the resistance and are not just secondary effects which maintain it, cetuximab sensitive (HN)SCC cells are generated and chromatin remodelers knocked down prior to the treatment. Comparing these knock-down constructs with cells, transfected with control constructs, would give us information whether resistance formation is delayed, impaired or increased in the absence of the epigenetic pathways. However, in the future it would be important to include human patient samples into the study and focus on the analysis of chromatin patterns, especially in terms of candidate gene expression. If those candidate genes were identified, it would be important to functionally test their role in the acquired resistance by overexpression or knock-down in the HNSCC cells. Additionally, cetuximab-resistant and -sensitive HNSCC patients could be analyzed, both testing whether the candidate genes found using the cell lines may serve as biomarkers. Thus, answering the question whether similar gene expression patterns can be found in cetuximab resistant patients. This would also be confirmed on a genome wide level performing NGS, to the end of providing personalized medical treatment for HNSCC patients.

4.3 Role of the VEGF signaling pathway in acquired resistance to cetuximab

Cancer cells rely on several, sometimes redundant activation pathways. Thus, EGFR is only one of them. The risk of treatment failure is real, if only one receptor is targeted. It

is known that EGFR mediated pathways are involved in tumor angiogenesis through the up-regulation of VEGF as well as other mediators of angiogenesis (Goldman et al., 1993). Accordingly, Lichtenberger et al. (2010) showed that autocrine VEGF signaling together with EGFR in tumor cells promotes development of epithelial tumors. Figure 22 shows the model of K5-SOS/EGFR-mediated tumorigenesis via ERK-dependent up-regulation of NRP1, FLT1 and VEGF expression, which leads to autocrine tumor cell proliferation via the VEGF/FLT1 signaling pathway (Lichtenberger et al., 2010)
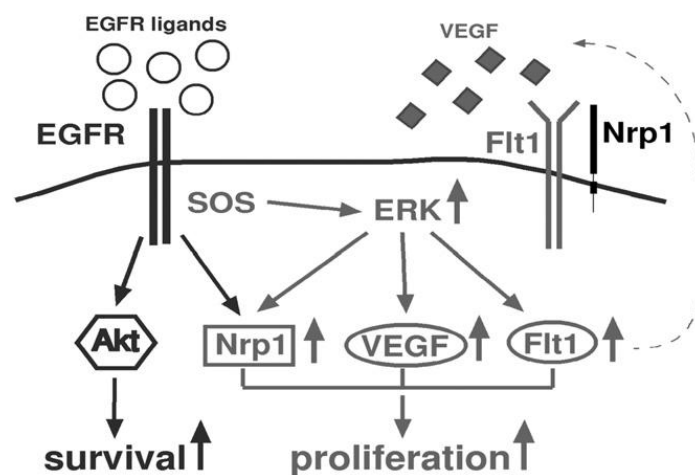

Figure 22: Autocrine VEGF signaling synergizes with EGFR in tumor cells to promote epithelial cancer development. Adapted from Lichtenberger et al., 2010.

Building on this results, I checked the gene expression of *EGFR* as well as of genes, which are involved in VEGF signaling in the cetuximab-sensitive and –resistant cell lines. The RNA Sequencing results revealed that *EGFR*, *VEGFA* (top up-regulated gene in both resistant cell lines) and *VEGFC* were up-regulated and *FLT1* down-regulated in the cetuximab-resistant cell line HNSCC22 R. *EGFR*, *VEGFA* and *FLT1* were up-regulated in the cell line SCC13 R. According to Bianco et al. (2008) the detection of FLT1 on tumor cells may indicate their increased ability to survive, invade and escape the inhibition of cetuximab. In line with this it was shown that up-regulation of tumor angiogenesis-promoting growth factors is a potential mechanism by which tumor cells evade the effects of EGFR-inhibition (Ciardiello et al., 2006; Viloria-petit et al., 2001). The enhanced expression of *VEGF* is involved in the "angiogenic switch" and associated with increased neovascularization within the tumor. This effect is triggered through several mechanisms; most importantly hypoxia (Folkman, 2007; Fontanini et al., 1997; Melillo, 2007). It was shown that treatment of several EGFR-expressing tumor cells with

cetuximab led to down-regulation of different mediators of angiogenesis (Dempke and Heinemann, 2009). Due to the complexity of the multiple intracellular signaling pathways, it is important to interfere at different stages to avoid escape mechanisms for the cancer cell (Ciardiello et al., 2006). Thus, combining molecular therapies targeting different survival pathways, such as anti-VEGF monoclonal antibodies or VEGFR2 inhibitors, with EGFR-inhibitors may result in potential benefit for cancer patients. This therapy approach is highly appealing with regard to research results showing that the angiogenic process is involved in the development of resistance to anti-EGFR therapy and thus a possible strategy to overcome acquired resistance to EGFR inhibitors. Supporting this result, Benavente et al. (2009) showed, that plugs with acquired resistance to cetuximab exhibit a higher vessel density than parental cells, by using matrigel plug neovascularization assay. In addition to our results, indicating that *VEGFA* is overexpressed in cetuximab resistant (HN)SCC cell lines, Viloria-petit et al. (2001) showed that *VEGF* expression was elevated in cetuximab-resistant A431 cells developed *in vitro*. Consequentially, as mentioned before, up-regulation of *VEGF* may contribute to increased angiogenesis and to resistance to cetuximab. To test this hypothesis, the treatment of cetuximab-resistant tumor cells by combining an EGFR targeting agent and the VEGF receptor targeting agent ZD6474 was evaluated (Ciardiello et al., 2004). The results showed that the combined treatment led to significantly greater tumor growth inhibition in both sensitive and resistant tumor cells. Relating to these results, I performed a MTT assay, in which cetuximab-sensitive cells were treated with cetuximab and VEGF simultaneously (Figure 21), expecting that the cetuximab-sensitive cells would lose sensitivity against the drug. Surprisingly, the results showed that VEGF in the culture medium of cetuximab-sensitive cells increased the inhibitory effect of cetuximab resulting in a dose-dependent decrease of cell growth with increasing concentrations of cetuximab. In order to gain a detailed understanding of the supportive function of VEGF regarding inhibition of cetuximab and whether it plays a role in the acquired resistance against the drug, it would be interesting to perform functional analyses to investigate how VEGF sensitizes tumor cells against the inhibitor. Foremost, it would be of particular interest to monitor when the high levels of *VEGF*, observed in cetuximab-resistant cell lines, can be first observed during the process of generating these cells. Therefore, the gene expression of *VEGF* would be analyzed after every doubling of cetuximab concentration. Furthermore, to get a clearer picture about the complexity of the multiple intracellular signaling pathways, different downstream signaling pathways,

especially the crosstalk of EGFR and VEGF, would be analyzed by performing immunoblotting analysis. Thus, the downstream signaling cascade of VEGF would be analysed after cetuximab treatment as well as the EGFR signaling cascade after treatment with an VEGF(R)-inhibitor. Furthermore, the effect of a combined treatment with these inhibitors would be analyzed on both pathways, as well as on the downstream signaling cascade of other pathways such as the NF-κB pathway, as it also plays a role in the progression of HNSCC (Chen et al., 2008; Pries et al., 1998). It is known that the activation of VEGF signaling results in the activation of different signaling cascades leading to cell proliferation, migration as well as cell survival (Byrne et al., 2005). For this reason it was surprising that VEGF resulted in decreased cell growth in the respective cell lines. To better understand the effect of cetuximab and VEGF on the cell growth, the proliferation as well as apoptosis of cetuximab-sensitive cell lines after exposure to the single reagents or in combination would be analyzed in proliferation and apoptosis assays. The proposed experiments would reveal how VEGF increases the effect of cetuximab on cancer cells.

5 Materials and Methods

5.1 Materials

5.1.1 Equipment

Machine	Model and Producer
Bioruptor	Bioruptor Plus, Diagenode
Cell culture microscope	Nikon TMS
Centrifuges	Centrifuge 5415C; Eppendorf Microcentrifuge 5415R; Eppendorf
Incubator (37°C)	Heraeus HERAcell; Kendro Laboratory Products
Laminar flow	VFR 1806; Thermo Fisher Scientific
Magnetic stirrer	RCT basic IKAMAG, IKA
pH meter	Meter Lab PHM210 standard pH Meter, Radiometer Copenhagen
Serological Pipettes	TPP Techno Plastic Products AG
Thermomixer	Thermomixer compact, Eppendorf
Vortexer	Reax top, Heidolph
Waterbath	GFL; Großhandel mit Laborgeräten

5.1.2 Chemicals and reagents

Reagent	Company
Cell culture grade water	S15-012 PAA Laboratories
DMEM	E15-810; PAA Laboratories
DMSO	1.09678.0100; Merck
dNTPs	U1240; Promega
ECL Western Blotting Detection Reagents	RPN2106; GE Healthcare Life Sciences

Ethanol	UN1170, VWR
FCS	A15-101; PAA Laboratories
Isopropanol	1.09634.1011; Merck
L-Glutamin 200mM	M11004: PAA Laboratories
MgCl2	2189.1; Roth
NaCl	3957.1; Roth
Penicillin/Streptomycin (Pen/Strep)	P11-010; PAA Laboratories
PBS (1X)	H15-002; PAA Laboratories
Proteinase K	03115879001; Roche
SDS solution 20%	161-0418, BIO RAD
TRIzol® Reagent	15596-018, Invitrogen
Trypsin	27250-018; Invitrogen

5.1.3 Commercialized test systems (Kits)

Click-iT® EdU Flow Cytometry Assay Kits	C10424; Invitrogen
EpiTect Bisulfite Kit	59104; Qiagen
In situ Cell Death Detection Kit, POD	11 684 817 910; Roche
RNeasy MinElute® Cleanup Kit	74204; Qiagen
NEBNext® DNA Library Prep Reagent Set for Illumina®	E6000S; NEB
NEBNext® mRNA Library Prep Reagent Set for Illumina®	E6100S; NEB
RNeasy® Mini Kit	74104; Qiagen
Vybrant® MTT Cell Proliferation Assay Kit	V-13154; Invitrogen

5.1.4 Media, Buffer and Solutions

10X Annexin V Binding Buffer	0,1M Hepes/NaOH (pH 7,4) 1,4M NaCl, 25mM $CaCl_2$ For a 1X working solution, 1 part of the 10X Annexin V Binding Buffer was diluted to 9 parts of ddH_2O
50x TAE-buffer	2 M Tris Acetate, 50 mM EDTA, pH 8,0

Dulbecco´s Modified Eagle´s Medium (DMEM)	580 mg/l L-Glutamine; 4,5 g/l D-Glucose; 3,7 g/l NaHCO$_3$; 8 mg/l Phenolred
Fetal bovine serum (FBS)	Inactivation for 30 min at 56 °C in waterbath
2x Freezing medium	4x FCS, 1x DMSO, filtered sterile
Glutamin	
Penicillin/Streptomycin (Pen/Strep)	10.000 U/10.000 µg/ml, filtered sterile
Phosphate Buffered Saline (PBS)	1x, in ddH$_2$O
RIPA buffer	50mM Tris, 150mM NaCl, 0,1% SDS, 0,5% sodium deoxycholate, 1% Triton X 100, cocktail protease inhibitors, PMSF
SCC medium	DMED high glucose (4,5 g/l D-Glucose), 10% FCS, Glutamine (100x), Pen/Strep (100x), Non-essentail amino acids (100x), 5 µg/ml Insulin (Sigma #15550), 10 µg/ml Transferrin (Sigma #T8158)
SCC starvation medium	DMED high glucose (4,5 g/l D-Glucose), 0,5% FCS, Glutamine (100x), Pen/Strep (100x), Non-essentail amino acids (100x)
Stripping buffer	31,25 mL 1M Tris (pH 6,8); 50 ml 20% SDS; 418,75 ml dH$_2$O

5.1.5 Cell culture-consumable material

The consumable material in the cell culture was ordered from the following companies:

Becton-Dickinson, Falcon (Heidelberg); Greiner Bio-One (Solingen) Nunc (Roskilde, Denmark);

5.1.6 Cell lines

The human SCC cell lines SCC13 as well as the human HNSCC cell lines HNSCC11 and HNSCC22 were kindly provided by Gian-Paolo Dotto and cultured in DMEM supplemented with 10% FBS (Sigma), L-glutamine (Sigma), penicillin (100 units/ml) and streptomycin (100 μg/ml), transferrin and insulin.

5.1.7 Antibodies

5.1.7.1 Primary antibodies

Cell Signaling

EGF Receptor (D38B1) XP® Rabbit mAb #4267(1:1000)

Phospho-EGF Receptor (Tyr1068) (D7A5) XP® Rabbit mAb #3777 (1:1000)

Phospho-p44/42 MAPK (Erk1/2) (Thr202/Tyr204) Antibody #9101(1:5000)

Santa Cruz

ERK 1 Antibody (C-16): sc-93

ERK 2 Antibody (C-14): sc-154

Sigma

Anti-Actin antibody produced in rabbit – A2066 (1:1000)

5.1.7.2 Secondary antibodies

Jackson Immuno

HRP goat anti-rabbit IgG – 111-035-003

5.1.8 Primer

Gene	sequence
hCBX2 F	gcaagctggagtacctggtc
hCBX2 R	ggctcccagctgttatgttt
hDNMT1 F	cccaagtaactgggattagagc
hDNMT1 R	ggtttgcctggtgcttttc
hDUSP6 F	cgactggaacgagaatacgg
hDUSP6 R	ggagaactcggcttggaact
hEGFR F	gccttgactgaggacagca
hEGFR R	tttgggaacggactggttta
hEZH1 F	cctgttctgctgttgtgtcc
hEZH1 R	ggatttggtatttccatcttgc
hEZH2 F	tgtggatactcctccaaggaa
hEZH2 R	gaggagccgtcctttttca
hFOS F	ctaccactcacccgcagact
hFOS R	aggtccgtgcagaagtcct

hFOSB F	gagctgaccgaccgactc
hFOSB R	ccgactccagctctgcttt
hIFI27 F	ccaagcttaagacggtgagg
hIFI27 R	ccgtggcctagagagtaagaga
hJMJD3 F	cctcgaaatcccatcacagt
hJMJD3 R	gtgttcgccactcgcttc
hJMJD7-PLA2G4B F	ggcaacctaccagctaactgaa
hJMJD7-PLA2G4B R	aggtcctggacacctctgc
hJUN F	ccaaaggatagtgcgatgttt
hJUN R	ctgtccctctccactgcaac
hKLRK1 F	ggcttttatccacaagaatcaag
hKLRK1 R	tctaaagtcttcaatgcacaaagg
hKRT81 F	agagcaacagctgagaacgag
hKRT81 R	gtctgacttgcggaggtagg
hMYC F	gctgcttagacgctggattt
hMYC R	taacgttgaggggcatcg
hPI3 F	tgatcgtggtggtgttcct
hPI3 R	acggcctttgacagtgtctt
hS100A7 F	ccaaacacacacatctcactca
hS100A7 R	tcagcttgagtgttgctcatc
hSOS1-2 F	ctagtaggaagctgctttgaagact
hSOS1-2 R	aaaatatctcgagcatacgattca
hSUVAR39 F	catggagtacgtgggagagat
hSUVAR39 R	cctgacggtcgtagatctgg
hTBP F	cggctgtttaacttcgcttc
hTBP R	cacacgccaagaaacagtga
hTOX2 F	gtgacgtgtccaaaatcgtg
hTOX2 R	tttgctgcttctgtcttcctc
hUTX reatime F	catgaacacagcacagcaga
hUTX realtime R	accatgaatgagcttgttgct
hVEGFA F	tgcccgctgctgtctaat
hVEGFA R	tctccgctctgagcaagg
hZNF177 F	ggaaggaaacctacaggagga
hZNF177 R	tcctggaaggttactgagttctg

5.1.9 EGFR-Inhibitors

Cetuximab by Merck (Merck Pharma GmbH, Darmstadt, Germany) was kindly provided by Univ. Prof. Dr. Walter Berger.

5.1.10 Statistics

Statistical analysis was performed using two-sided Student´s t-test.

$p < 0,05$ (∗)

$p < 0,001$ (∗∗)

5.2 Cell culture of human squamous cell carcinoma cell lines

5.2.1 Cultivation and passage of SCCs

After thawing, the cells were cultured for two passages. Afterwards, the concentration of the cells was measured and $1x10^5$ cells were seeded in 6-well plates.

5.2.2 Cryoconservation of SCCs

To extend the viability of SCCs over several years, cells are frozen into liquid nitrogen. This procedure is designated as cryoconservation and is performed as follows: The cells are washed with 1xPBS and trypsinized for 30 min. After that, the cells are transferred into SCC medium. 1 part of the cell suspension is mixed with 1 part 2x freezing medium. The cells are immediately stored on -80°C.

5.2.3 Thawing of SCCs

For the thawing of SCCs 5ml of the SCC culture medium was prewarmed. At the same time the cryo vial containing the SCC cells was taken out of the -80°C freezer and given into a 37°C water bath. After 2 min the cells were thawed and transferred immediately to the prewarmed medium. The cells were centrifuged at 1000 rpm for 5 min. Furthermore, the supernatant was discarded and the pellet was resuspended in 10 ml SCC culture medium, seeded onto a 10 cm culture dish and incubated in an incubator at 37°C and 5% CO_2-fumigation. After the 2nd cell passage the cells were suitable for further experiments.

5.2.4 Determination of cell concentration

For the determination of the cell concentration the cells were resuspended in SCC medium. Furthermore, 5 ml of CASYton was mixed with 5 μl of the cell suspension. After that, the concentration was measured.

5.2.5 Establishment of acquired resistance to the EGFR inhibitor cetuximab

Over a period of 10 weeks, tumor cells in culture were continuously exposed to increasing concentrations of cetuximab. Commencing with the IC_{50}% of cetuximab, the exposure dose was doubled every 14 days. The treatment was performed with two different starting concentrations (low treatment (2,5 μg/ml) and high treatment (5 μg/ml). $5*10^4$ cells of the particular cell line were seeded in a 6-well plate and treated with cetuximab for 3 days. After that, the cells were cultured for 3 days w/o cetuximab.

The cells were splitted, plated on a new 6-well plate at the initial density and the treatment was started again one day after passaging the cells. The established resistant cell lines were maintained in continuous culture with the maximally achieved dose of EGFR inhibitor, in our case 40 µg/ml, that still allowed cellular proliferation. In parallel, parental cells were cultured without cetuximab.

5.2.6 Examination of receptor inhibition by cetuximab

For the examination of the efficacy of cetuximab treatment, 1x 10^5 cells of the respective cell clone were seeded in 6-well plates. The cells were treated with different conditions.
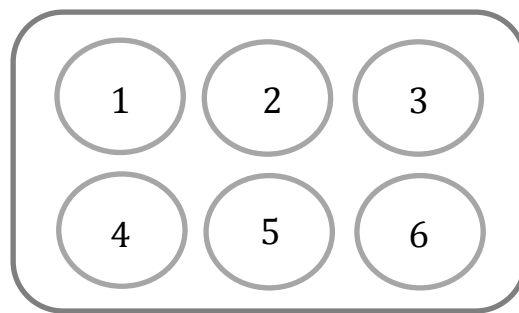
The medium was changed in all wells. However, in well 1 SCC medium was given, whereas in well 2-6 the cells were treated with starvation medium. The cells were incubated at 37 °C o/n. The next day, cetuximab was added to well 4-6 in the following concentrations:

4) Cetuximab 10 µg/ml

5) Cetuximab 100 µg/ml

6) Cetuximab 1000 µg/ml

The 6-well plate was stored on 37 °C for 1 h. After that, 8 µl EGF (250x; Roche) was added. Another incubation step at 37 °C for 20 min followed. The cells were harvested using the protein isolation protocol.

5.3 Molecular biology

5.3.1 RNA-Isolation using TRIzol

The total RNA was isolated with TRIzol Reagent (Invitrogen). Therefore, the cells were washed once with 1x PBS. Furthermore, 500 µl of TRIzol was given on the cells. These were harvested and transferred into a tube. 200 µl of chloroform was added and the tube was vortexed for 10 sec. A centrifugation step followed at 14.000 rpm for 10 min.

The upper aqueous phase containing the RNA was transferred into a new tube and mixed with 0,6 volumina isopropanol. It was centrifuged at 13.300 rpm for 30 min at 4 °C. After that, the supernatant was discarded and the pellet was washed with 100 μl 70% ethanol. Another centrifugation step followed at 13.300 rpm for 10 min at 4°C. The supernatant was discarded and the pellet was dried for 15 min. After that, the pellet was resuspended in 150 μl of cell culture water. The quality of the RNA was controlled by OD260/280 nm analysis on a Nanodrop (Thermo Fisher Scientific, Landsmeer, The Netherlands).

5.3.2 c-DNA synthesis

For the c-DNA synthesis the RNA concentration was measured. 500ng of RNA was used for one reaction. The reaction was performed in a total volume of 20μl:

Reagents	Volume
5x FS buffer	4μl
Random hexamers	2μl
DTT 0,1M	2μl
dNTPs	1μl
SSRT	0,5μl
RNA (500ng)	X μl
ddH$_2$O	X μl
total volume	20 μl

The samples were stored on 42°C for 50min. After that, an inactivation step followed at 70°C for 10 min. 30 μl of cell culture water were added to each reaction.

5.3.3 Quantitative Real-Time-PCR (qRT-PCR) analysis

Amplification of the c-DNA was performed on the ABI/Prism 7000 Sequence Detector System. For each sample the Ct-value, the cycle number at which the amount of amplified target crossed a pre-determined threshold, was determined. To correct for differences in RNA input, TATA-binding protein (TBP) was used as a reference gene for each RNA sample. The quantitative real-time PCR analysis reaction was performed in a total volume of 20 μL:

Reagents	Volume
SYBR green master mix (2x)	10μl
Primer (1:10)	2μl

cDNA sample	1µl
ddH$_2$O	7µl
Total volume	20 µl

5.4 Immunoblotting analysis

5.4.1 Protein isolation

Cells were washed once with 1x PBS. After that, RIPA-buffer containing protease inhibitor cocktail (1:100), PMSF (1:100), 200 mM NaVO$_3$ (200x) and 1M NaF (40x) was given on the cells. The plate containing the cells was stored on 4 °C for 10 min. The cells were harvested and sonicated in the Bioruptor with 3 cycles (30 ON, 90 OFF). A centrifugation step at full speed and 4°C for 15 min followed. The supernatant was transferred into a new tube.

5.4.2. SDS-PAGE and western blot analysis

The protein concentration was measured using the Bradford protein assay. Normally, 50 µg of protein were analyzed by SDS-PAGE. In case of smaller protein concentration 25 µg of protein were loaded. The gel was run over night at 32V. After that, the separated proteins were transferred to nitrocellulose membranes. For the transfer, the membrane was equilibrated in methanol and washed with cell culture water. The transfer was performed for 3 h and 30 min. The membrane was washed with water and Ponceau S was given on the membrane to check for successful transfer. The membrane was washed with cell culture water and after that with 1x TBS-T. In the next step, the membrane was blocked with 5% milk in TBS with 0,5% Tween 20 (TBS-T). The membranes were incubated with the primary antibody in 5% milk in TBS-T overnight at 4°C. They were washed thrice with TBS-T for 5-10 min and incubated with an HRP-coupled anti-rabbit and anti-mouse secondary antibody (1:5000) in 5% milk in TBS-T for 1 h at room temperature. The membranes were washed thrice with TBS-T for 5-10 min each and the protein bands were visualized using the enhanced chemiluminescent (ECL) method (GE Healthcare).

5.4.3. Stripping and reprobing

For stripping of the membrane, 50 ml of the stripping buffer was mixed with 360µl ß-mercaptoethanol. The membrane was given in this solution and incubated for 20 min at 55°C in a water bath with agitation. After that, the membrane was given into TBS-T for 30 min and could be used for the blocking stage.

5.5 Assessment of apoptosis

5.5.1 Apoptosis assay

Apoptosis was detected by flow cytometry via the examination of altered plasma membrane phospholipid packing by lipophilic dye Annexin V. Therefore, the FITC Annexin V staining protocol was performed. In this assay Annexin V as a FITC conjugate in combination with 7-AAD as an exclusion dye for cell viability, detects apoptotic cells and discriminates between apoptosis and necrosis. Annexin V is a calcium-dependent phospholipid-binding protein that has a high affinity for phosphatidylserine (PS). The cells were washed twice with cold PBS and resuspended in 1X Binding Buffer at a concentration of 1×10^6 cells/ml. 100 μl of the solution (1×10^5 cells) was transferred to a FACS tube. 5μl of Annexin V as well as 4μl of 7-AAD were added. The cells were vortexed gently and incubated for 15 min at RT (25 °C) in the dark. After that, 400 μl of 1X Binding Buffer was added to each tube. The analysis was performed by flow cytometry within 1 hr. All early apoptotic cells (Annexin V-positive, 7-AAD negative), necrotic/late apoptotic cells (double positive) and living cells (double negative) were detected by FACSCalibur flow cytometer and analyzed by Cell Quest software (Becton Dickinson).

5.5.2 *In situ* cell death detection kit, POD

The cells were seeded in 6-well plates on cover slips which were coated with Poly-D-lysine for 30 min at 37°C. After 24 h and 48 h 40 μg/ml of cetuximab was added to the cells. The next day, the protocol was performed analogous to the instructions of the kit. A positive as well as a negative control was included in the experiment. In the positive control, the cells were treated with DNAse I for 10 min to induce double strand breaks. In the negative control, the cells were treated with the labeling solution w/o the enzyme.

5.6 MTT cell proliferation assay

The cell proliferation assay was performed using the Vybrant MTT cell proliferation assay kit. During the assay the water soluble MTT (3-(4,5-dimethylthiazol-2-yl)-2,5-diphenyltetrazolium bromide) is converted to an insoluble formazan. The formazan is then solubilized and the concentration determined by optical density at 570nm. First, the cells are seeded in a 96-well plate at a density of 3000 cells per well. After 24 and 48 hours, increasing concentrations of cetuximab were added (2,5μg/ml, 5μg/ml, 10μg/ml and 25μg/ml). In parallel, cells were cultured without cetuximab. After 72 hours, the

medium was removed and replaced with 100µl of fresh culture medium. 10µl of the 12mM MTT stock solution was added to each well. By that, a negative control was included by adding 10µl of the MTT stock solution to 100µl of medium alone. The cells were incubated at 37°C for 4 hours. After that, 100µl of the SDS-HCl solution were added to each well and the solution was mixed thoroughly. The plate was incubated at 37°C overnight. Each sample was mixed again and the absorbance was read at 570nm.

5.7 EdU Flow Cytometry Assay

5×10^4 cells were seeded in 6-well dishes for 24 h at 37°C. At 40% confluency the cells were left untreated or treated with cetuximab (40µg/ml). The cells were pulsed with 5 µM EdU for 8 h and 16 h. After that, the protocol of the Click-iT EdU Flow Cytometry Assay Kit was followed. The number of proliferating cells was analyzed on a LSR-II Flow cytometer.

5.8 Assay of tumor growth in athymic nude mice

The cells were seeded in 6 cm dishes. After three days, the cells were washed with 1x with 1xPBS. A trypsinization process followed. The cells were resuspended in 1x PBS and given over a 70µm cell strainer. After that, the concentration was measured. The human cancer cell lines (1×10^6 cells) were injected subcutaneous into the dorsal flank area of the mice. The tumor volume was determined by direct measurement with calipers and calculated by the formula: π/6 x (large diameter) x (small diameter).

5.9 NEB Next DNA library

End repair of fragmented DNA

6 µg of DNA was mixed with 0,5% unmethylated λ DNA. The samples were sonicated with 20 cycles (30 ON/30 OFF). After that, the ends of the fragmented DNA were repaired.

Reagents	Volume
Fragmented DNA (+λ DNA)	85 µl
NEB Next End Repair Reaction buffer (10X)	10 µl
NEB Next Repair Enzyme Mix	5 µl
Total volume	100 µl

The samples were stored at 20°C for 30 min.

Clean up using AMPure beads

The DNA was cleaned up using AMPure XP Beads. Therefore, the beads were vortexed and 1,6 volumina of the beads were added to the ligation reaction. The reaction was mixed thoroughly on a vortex mixer. An incubation step at RT for 5 min. followed. The tubes were put in a magnetic stand to separate the beads from the supernatant. After the solution was clear (5 min.) the supernatant was removed and discarded. Thereby, the beads containing the DNA targets were not disturbed. 200 µl of 80% freshly prepared ethanol was added to the tubes while the tubes were in the magnetic stand. It was incubated at RT for 30 sec. After that, the supernatant was removed and discarded. The step was repeated and the beads were air-dried for 10 min. while the tubes were on the magnetic stand with the lid open. The DNA target was eluted by adding 44 µl sterile water to the beads. It was pipetted up and down and the tubes were put on a magnetic stand until the solution was clear (2 min.).

dA-Tailing of End Repaired DNA

In the next step dA-Tailing of end repaired DNA was performed.

Reagents	Volume
End Repaired, Blunt DNA	42 µl
NEB Next dA-Tailing Reaction Buffer (10x)	5 µl
Klenow Fragment (3´->5´ exo-)	3 µl
Total volume	50 µl

After this step, another clean up step followed (see **Clean up using AMPure beads**). The DNA target was eluted by adding 27 µl sterile water to the beads.

Adaptor Ligation of dA-Tailed DNA

Reagents	Volume
dA-Tailed DNA	25 µl
Quick Ligation Reaction Buffer (5x)	10 µl
15µM DNA Adaptors	10 µl
Quick T4 DNA Ligase	5 µl
Total volume	50 µl

The following adaptors were used:

Set A

Sample	Library Adapter	Barcode Sequence
13 S	Illumina TruSeq AD005	ACAGTG
13 R	Illumina TruSeq AD006	GCCAAT
22 S	Illumina TruSeq AD015	ATGTCA
22 R	Illumina TruSeq AD013	AGTCAA

Another clean up step followed analogous to **Clean up using AMPure beads**. However, this time the DNA target was eluted by adding 102 µl sterile water to the beads for bead-based size selection. 100 µl of the supernatant was transferred to a new tube. The bead-based size selection followed.

Size select adaptor ligated DNA using AMPure XP beads

80 µl (0,8x) resuspended AMPure XP beads was added to 100 µl DNA solution. The solution was pipetted up and down for at least 10 times. Furthermore, it was incubated at RT for 5 min. The tubes were put on a magnetic stand to separate the beads from the supernatant. After 5 min. the solution was clear and the supernatant was transferred carefully to a new tube. The beads containing the large fragments were discarded. Furthermore, 20 µl (0,2x) of the resuspended AMPure XP beads was added to the supernatant, it was mixed well and incubated at RT for 5 min. The tubes were put on an appropriate magnetic stand to separate beads from the supernatant. After 5 min. the solution was clear and the supernatant was carefully removed and discarded. Thereby, the beads that contained the DNA targets were not disturbed. The protocol was performed analogous to 3.6.2 by adding 200 µl of freshly prepared 80% ethanol, however this time in the end the DNA target was eluted from the beads into 22 µl of sterile water. It was pipetted up and down and the tube was put on the magnetic stand until the solution was clear. 20 µl of the supernatant was used for the enrichment.

Bisulfite treat ligation products

Reagent	Volume
DNA sample	20 µl
Bisulfite mix	85 µl
DNA protection buffer	35 µl
Total volume	140 µl

The total volume of 140 µl was split à 2x 70 µl. The following PCR program was used.

Procedure	Temperature (°C)	Time (min)
Denaturation	95	5
Incubation	60	25
Denaturation	95	5
Incubation	60	85
Denaturation	95	5
Incubation	60	175
Denaturation	95	5
Incubation	60	180
Hold	20	Indefinite

Cleanup bisulfite converted DNA

For the cleanup the samples were pooled. The protocol was performed analogous to the instructions of the EpiTect Bisulfite handbook. The purified DNA was eluted in 2x 20 µl nuclease-free water. After that, the DNA was pooled. 80 µl of the AMPure XP beads was added and the protocol was performed analogous to **Clean up using AMPure beads**. The DNA was eluted in 23 µl nuclease-free water. After that, the concentration was measured.

Enrich DNA fragments

Reagents	Volume
DNA	10 µl
Ultrapure H_2O	27,75 µl
Pfu Turbo Cx Reaction buffer	5 µl
10mM dNTP mix	1,25 µl
PCR primer cocktail	5 µl
Pfu Turbo Cx Hotstart DNA Polymerase	1 µl
Total volume	50 µl

The following PCR program was used

Procedure	Temperature (°C)	Time (sec)
Initial denaturation	95 98	300 30
Denaturation	98	10
Annealing	65	30
Extension	72	30
Final Extension	72 4	300 Indefinite

After the enrichment, the samples were pooled and 100 µl of the beads were added. Furthermore, the cleanup step was performed analogous to **Clean up using ampure beads.** The DNA was eluted in 23 µl nuclease-free water.

5.10 NEB Next mRNA library

For the cleanup of the RNA 4 µg of the samples were used. The protocol was performed analogous to the instructions of the "RNA cleanup" protocol of the RNeasy Mini kit. The RNA was eluted in 50 µl RNAse-free water. Furthermore, the protocol of the NEB Next mRNA library Instruction manual was performed. 250 ng of the purified mRNA was used as starting material.

mRNA fragmentation protocol

Reagent	Volume
Purified mRNA	18 µl
10x RNA fragmentation reaction buffer	2 µl
Total volume	20 µl

The samples were stored at 94°C for 5 min to generate 200 nucleotide RNA fragments. After that, the tubes were transferred to ice. 2 µl of the 10x RNA Fragmentation Stop solution was added. Furthermore, 78 µl of nuclease-free water was added and the samples were purified analogous to the protocol described in the MinElute Cleanup Kit. The RNA was eluted in 15,5 µl NFW. The column purification removes short RNA fragments and enriches the sample for RNA fragments longer than 200 nucleotides.

First Strand cDNA synthesis

The following components were mixed in a sterile PCR tube:

Reagents	Volume
Fragmented mRNA	13,5 µl
Random Primers	1 µl
Total volume	14,5 µl

The samples were incubated at 65°C for 5 min. Furthermore, the tubes were spun briefly and placed on ice. To the fragmented mRNA and random primers the following reagents were added:

Reagents	Volume
5x first strand synthesis reaction buffer	4 µl
Murine RNase Inhibitor	0,5 µl
Total volume	19 µl

The samples were incubated at 65°C for 2 min. 1 µl of M-MuLV Reverse Transcriptase (RNase H$^-$) was added to the reaction. The samples were incubated as follows:

Time (min)	Temperature (°C)
10	25
50	42
15	70
Indefinite	4

Second strand synthesis

The following reagents were added to the first strand synthesis reaction:

Reagents	Volume
Nuclease-free water	48 µl
10x Second strand synthesis reaction buffer	8 µl
Second strand synthesis enzyme mix	4 µl
Total volume	80 µl

The samples were mixed by gentle pipetting and incubated in a thermal cycler for 2.5 h at 16 °C. The double-stranded cDNA was purified using 1,8x Agencourt AMPure XP beads. The beads were vortexed to resuspend the beads. Furthermore, 1,8x of the beads was added to the second strand synthesis reaction (80 µl). After that, the protocol was performed analogous to **Clean up using AMPure beads.** The DNA target was eluted from the beads into 52 µl water. 50µl of the clear solution was transferred to a clean 1.5 ml LoBind® (Eppendorf AG) tube.

End repair of cDNA library

The following components were mixed:

Reagents	Volume
Purified double-stranded cDNA	50 µl
Nuclease-free water	25 µl
10x Phosphorylation reaction buffer	10 µl
Deoxynucleotide Solution Mix	4 µl
T4 DNA Polymerase	5 µl
E. coli DNA Polymerase I, Large (Klenow) Fragment	1 µl
T4 Polynucleotide Kinase	5 µl
Total volume	100 µl

The samples were incubated in a heat block at 20°C for 30 min.

The end-repaired cDNA was purified using 1.8x AMP XP beads (**Clean up using AMPure beads**). The DNA target was eluted from the beads into 34 µl water. 32 µl of the clear solution was transferred to a clean 1.5 ml LoBind tube.

dA-Tailing of cDNA Library

The following components were mixed:

Reagents	Volume
Purified, End repaired cDNA	32 µl
NEBuffer2	5 µl
Deoxyadenosine 5´triphosphate (1mM)	10 µl
Klenow fragment (3´-> 5´ exo⁻)	3 µl
Total volume	50 µl

The samples were incubated in a heat block at 37°C for 30 minutes.

The dA-tailed DNA was purified using 1.8x AMPure XP beads analogous to **Clean up using AMPure beads.** The DNA target was eluted from the into 25 µl water for bead-based size selection. The solution was mixed by pipetting up and down. Furthermore, the tube was put in the magnetic stand until the solution was clear. The supernatant was removed and transferred to a clean 1.5 ml LoBind tube.

Adaptor Ligation of cDNA Library

The following components were mixed:

Reagent	Volume
Purified, dA-Tailed cDNA	23 µl

2x Quick Ligation Reaction Buffer	25 μl
NEBNext Adaptors (15μM)	1 μl
Quick T4 DNA Ligase	1 μl
Total volume	50 μl

The samples were incubated at RT for 15 min. Furthermore, 3 μl of USER™ enzyme was added and the samples were mixed by pipetting up and down and incubated at 37°C for 15 min. After that, a purification step followed analogous to **Clean up using AMPure beads.** 1,8X of the resuspended AMPure XP beads were added to the ligation reaction. The DNA target was eluted from the beads into 150 μl of NFW for bead-based selection.

Size selection of adaptor-ligated DNA

0,9x of the resuspended AMPure XP beads was added to 150 μl of the eluted DNA target. After mixing by pipetting up and down, the samples were incubated at RT for 5 min. The tube was placed on a magnetic stand. After the solution was clear the supernatant was transferred to a new tube. In this case, the beads containing the large fragments were discarded. 0.2x of the resuspended beads was added to the supernatant, mixed and incubated at RT for 5 min. The tube was put on the magnetic stand to separate the beads from the supernatant. After the solution was clear, the supernatant was discarded. 200 μl of freshly prepared 80% ethanol was added and the protocol was performed analogous to **Clean up using AMPure beads.** The DNA target was eluted from the beads into 25 μl NFW and 23 μl of the supernatant was transferred to a clean PCR tube.

PCR enrich adaptor ligated cDNA library

The following components were mixed:

Reagent	Volume
Size selected cDNA	23 μl
NEBNext High-Fidelity 2X PCR Master mix	25 μl
Universal PCR primer (25μM)	1 μl
Index primer (x) (25μM)	1 μl
Total volume	50 μl

Index primer

Sample name	Library adapter	Barcode sequence
13S	NEBNext Index 2 Primer for Illumina	CGATGT
13R	NEBNext Index 4 Primer for Illumina	TGACCA
22S	NEBNext Index 6 Primer for Illumina	GCCAAT
22R	NEBNext Index 12 Primer for Illumina	CTTGTA

PCR cycling conditions:

Cycle step	Temperature (°C)	Time (sec)	Cycles
Initial Denaturation	98	10	1
Denaturation **Annealing** **Extension**	98 65 72	10 30 30	12
Final extension	72 4	300 hold	1

The PCR product was purified analogous to **Clean up using AMPure beads.** 1.2x of the resuspended beads was added to the PCR reaction and the DNA target was eluted from the beads into 22,5 µl TE buffer. 20 µl of the supernatant was transferred to a 1,5 ml LoBind tube and stored at -20°C.

6 References

Arteaga, C.L. (2003). EGF receptor as a therapeutic target: patient selection and mechanisms of resistance to receptor-targeted drugs. Journal of Clinical Oncology : Official Journal of the American Society of Clinical Oncology *21*, 289s–291s.

Bardelli, A., and Jänne, P. a (2012). The road to resistance: EGFR mutation and cetuximab. Nature Medicine *18*, 199–200.

Baselga, J. (2001). The EGFR as a target for anticancer therapy--focus on cetuximab. European Journal of Cancer (Oxford, England : 1990) *37 Suppl 4*, S16–22.

Batsakis, J. (1979). Tumors of the head and neck: clinical and pathological considerations.

Benavente, S., Huang, S., Armstrong, E. a, Chi, A., Hsu, K.-T., Wheeler, D.L., and Harari, P.M. (2009). Establishment and characterization of a model of acquired resistance to epidermal growth factor receptor targeting agents in human cancer cells. Clinical Cancer Research : an Official Journal of the American Association for Cancer Research *15*, 1585–1592.

Berdasco, M., and Esteller, M. (2010). Aberrant epigenetic landscape in cancer: how cellular identity goes awry. Developmental Cell *19*, 698–711.

Bianco, R., Troiani, T., Tortora, G., and Ciardiello, F. (2005). Intrinsic and acquired resistance to EGFR inhibitors in human cancer therapy. Endocrine-related Cancer *12 Suppl 1*, S159–71.

Bianco, R., Rosa, R., Damiano, V., Daniele, G., Gelardi, T., Garofalo, S., Tarallo, V., De Falco, S., Melisi, D., Benelli, R., et al. (2008). Vascular endothelial growth factor receptor-1 contributes to resistance to anti-epidermal growth factor receptor drugs in human cancer cells. Clinical Cancer Research : an Official Journal of the American Association for Cancer Research *14*, 5069–5080.

Bock, C., and Lengauer, T. (2008). Computational epigenetics. Bioinformatics (Oxford, England) *24*, 1–10.

Brand, T.M., Dunn, E.F., Iida, M., Myers, R. a, Kostopoulos, K.T., Li, C., Peet, C.R., and Wheeler, D.L. (2011a). Erlotinib is a viable treatment for tumors with acquired resistance to cetuximab. Cancer Biology & Therapy *12*, 436–446.

Brand, T.M., Iida, M., and Wheeler, D.L. (2011b). Molecular mechanisms of resistance to the EGFR monoclonal antibody cetuximab. Cancer Biology & Therapy *11*, 777–792.

Byrne, A.M., Bouchier-Hayes, D.J., and Harmey, J.H. (2005). Angiogenic and cell survival functions of vascular endothelial growth factor (VEGF). Journal of Cellular and Molecular Medicine *9*, 777–794.

Camp, E.R., Summy, J., Bauer, T.W., Liu, W., Gallick, G.E., and Ellis, L.M. (2005). Molecular Mechanisms of Resistance to Therapies Targeting the Epidermal Growth Factor Receptor Epidermal Growth Factor Receptor. 397–405.

Carmeliet, P. (2003). Angiogenesis in health and disease. Nature Medicine *9*, 653–660.

Chaisaingmongkol, J., Popanda, O., Warta, R., Dyckhoff, G., Herpel, E., Geiselhart, L., Claus, R., Lasitschka, F., Campos, B., Oakes, C.C., et al. (2012). Epigenetic screen of human DNA repair genes identifies aberrant promoter methylation of NEIL1 in head and neck squamous cell carcinoma. Oncogene *31*, 5108–5116.

Chen, S., Ma, J., Wu, F., Xiong, L.-J., Ma, H., Xu, W., Lv, R., Li, X., Villen, J., Gygi, S.P., et al. (2012). The histone H3 Lys 27 demethylase JMJD3 regulates gene expression by impacting transcriptional elongation. Genes & Development *26*, 1364–1375.

Chen, Z., Yan, B., and Van Waes, C. (2008). The Role of the NF-kappaB Transcriptome and Proteome as Biomarkers in Human Head and Neck Squamous Cell Carcinomas. Biomarkers in Medicine *2*, 409–426.

Chong, S., and Whitelaw, E. (2004). Epigenetic germline inheritance. Current Opinion in Genetics & Development *14*, 692–696.

Ciardiello, F. (2000). Epidermal growth factor receptor tyrosine kinase inhibitors as anticancer agents. Drugs *60 Suppl 1*, 25–32; discussion 41–2.

Ciardiello, F., and Tortora, G. (2008). EGFR antagonists in cancer treatment. The New England Journal of Medicine *358*, 1160–1174.

Ciardiello, F., Bianco, R., Caputo, R., Caputo, R., Damiano, V., Troiani, T., Melisi, D., Vita, F. De, Placido, S. De, and Bianco, A.R. (2004). Antitumor Activity of ZD6474 , a Vascular Endothelial Growth Factor Receptor Tyrosine Kinase Inhibitor , in Human Cancer Cells with Acquired Resistance to Antiepidermal Growth Factor Receptor Therapy. Clinical Cancer Research : an Official Journal of the American Association for Cancer Research *10*, 784-793

Ciardiello, F., Troiani, T., Bianco, R., Orditura, M., Morgillo, F., Martinelli, E., Morelli, M.P., Cascone, T., and Tortora, G. (2006). Interaction between the epidermal growth factor receptor (EGFR) and the vascular endothelial growth factor (VEGF) pathways: a rational approach for multi-target anticancer therapy. Annals of Oncology : Official Journal of the European Society for Medical Oncology / ESMO *17 Suppl 7*, vii109–14.

Citri, A., and Yarden, Y. (2006). EGF-ERBB signalling: towards the systems level. Nature Reviews. Molecular Cell Biology *7*, 505–516.

Cloos, J., Spitz, M.R., Schantz, S.P., Hsu, T.C., Zhang, Z.F., Tobi, H., Braakhuis, B.J., and Snow, G.B. (1996). Genetic susceptibility to head and neck squamous cell carcinoma. Journal of the National Cancer Institute *88*, 530–535.

Cooper, J.B., Eddy, E., and Cohen, W. (2009). Mechanisms of resistance to EGFR inhibitors in head and neck cancer. Head neck 1086–1094.

Cursiefen, C., Chen, L., Borges, L.P., Jackson, D., Cao, J., Radziejewski, C., D'Amore, P.A., Dana, M.R., Wiegand, S.J., and Streilein, J.W. (2004). VEGF-A stimulates lymphangiogenesis and hemangiogenesis in inflammatory neovascularization via macrophage recruitment. The Journal of Clinical Investigation *113*, 1040–1050.

Davies, R.L., Grosse, V. a, Kucherlapati, R., and Bothwell, M. (1980). Genetic analysis of epidermal growth factor action: assignment of human epidermal growth factor receptor gene to chromosome 7. Proceedings of the National Academy of Sciences of the United States of America *77*, 4188–4192.

Dempke, W.C.M., and Heinemann, V. (2009). Resistance to EGF-R (erbB-1) and VEGF-R modulating agents. European Journal of Cancer (Oxford, England : 1990) *45*, 1117–1128.

Diniz-Freitas, M., García-Caballero, T., Antúnez-López, J., Gándara-Rey, J.M., and García-García, a (2007). Pharmacodiagnostic evaluation of EGFR expression in oral squamous cell carcinoma. Oral Diseases *13*, 285–290.

Döbrossy, L. (2005). Epidemiology of head and neck cancer: magnitude of the problem. Cancer Metastasis Reviews *24*, 9–17.

Engelman, J. a, and Jänne, P. a (2008). Mechanisms of acquired resistance to epidermal growth factor receptor tyrosine kinase inhibitors in non-small cell lung cancer. Clinical Cancer Research : an Official Journal of the American Association for Cancer Research *14*, 2895–2899.

Esteller, M. (2006). Epigenetics provides a new generation of oncogenes and tumour-suppressor genes. British Journal of Cancer *94*, 179–183.

Esteller, M. (2007). Cancer epigenomics: DNA methylomes and histone-modification maps. Nature Reviews. Genetics *8*, 286–298.

Ezhkova, E., Pasolli, H.A., Parker, J.S., Stokes, N., Su, I., Hannon, G., Tarakhovsky, A., and Fuchs, E. (2009). Ezh2 orchestrates gene expression for the stepwise differentiation of tissue-specific stem cells. Cell *136*, 1122–1135.

Ferlay, J., Shin, H.-R., Bray, F., Forman, D., Mathers, C., and Parkin, D.M. (2010). Estimates of worldwide burden of cancer in 2008: GLOBOCAN 2008. International Journal of Cancer. Journal International Du Cancer *127*, 2893–2917.

Folkman, J. (2007). Angiogenesis: an organizing principle for drug discovery? Nature Reviews. Drug Discovery *6*, 273–286.

Fontanini, G., Vignati, S., Boldrini, L., Chinè, S., Silvestri, V., Lucchi, M., Mussi, a, Angeletti, C. a, and Bevilacqua, G. (1997). Vascular endothelial growth factor is associated with neovascularization and influences progression of non-small cell lung carcinoma. Clinical Cancer Research : an Official Journal of the American Association for Cancer Research *3*, 861–865.

Gandini, S., Botteri, E., Iodice, S., Boniol, M., Lowenfels, A.B., Maisonneuve, P., and Boyle, P. (2008). Tobacco smoking and cancer: a meta-analysis. International Journal of Cancer. Journal International Du Cancer *122*, 155–164.

Goldman, C., Kim, J., Wong, W., King, V., Brock, T., and Gillespie, G. (1993). Epidermal growth factor stimulates vascular endothelial growth factor production by human malignant glioma cells: a model of glioblastoma multiforme pathophysiology. Mol. Biol. Cell *4*, 121–133.

Goldstein, N.I., Prewett, M., Zuklys, K., Rockwell, P., and Mendelsohn, J. (1995). Biological efficacy of a chimeric antibody to the epidermal growth factor receptor in a human tumor xenograft model. Clinical Cancer Research : an Official Journal of the American Association for Cancer Research *1*, 1311–1318.

Hanahan, D., and Weinberg, R.A. (2011). Hallmarks of cancer: the next generation. Cell *144*, 646–674.

Harari, P.M. (2004). Epidermal growth factor receptor inhibition strategies in oncology. Endocrine-related Cancer *11*, 689–708.

Hashibe, M., Brennan, P., Benhamou, S., Castellsague, X., Chen, C., Curado, M.P., Dal Maso, L., Daudt, A.W., Fabianova, E., Fernandez, L., et al. (2007). Alcohol drinking in never users of tobacco, cigarette smoking in never drinkers, and the risk of head and neck cancer: pooled analysis in the International Head and Neck Cancer Epidemiology Consortium. Journal of the National Cancer Institute *99*, 777–789.

Herranz, M., and Esteller, M. (2006). New therapeutic targets in cancer: the epigenetic connection. Clinical & Translational Oncology : Official Publication of the Federation of Spanish Oncology Societies and of the National Cancer Institute of Mexico *8*, 242–249.

Hopkins, J., Cescon, D.W., Tse, D., Bradbury, P., Xu, W., Ma, C., Wheatley-Price, P., Waldron, J., Goldstein, D., Meyer, F., et al. (2008). Genetic polymorphisms and head and neck cancer outcomes: a review. Cancer Epidemiology, Biomarkers & Prevention : a Publication of the American Association for Cancer Research, Cosponsored by the American Society of Preventive Oncology *17*, 490–499.

Ichihashi, M., Ueda, M., Budiyanto, a., Bito, T., Oka, M., Fukunaga, M., Tsuru, K., and Horikawa, T. (2003). UV-induced skin damage. Toxicology *189*, 21–39.

Jaenisch, R., and Bird, A. (2003). Epigenetic regulation of gene expression: how the genome integrates intrinsic and environmental signals. Nature Genetics *33 Suppl*, 245–254.

Jenuwein, T., and Allis, C.D. (2001). Translating the histone code. Science (New York, N.Y.) *293*, 1074–1080.

Joukov, V., Pajusola, K., Kaipainen, a, Chilov, D., Lahtinen, I., Kukk, E., Saksela, O., Kalkkinen, N., and Alitalo, K. (1996). A novel vascular endothelial growth factor, VEGF-C, is a ligand for the Flt4 (VEGFR-3) and KDR (VEGFR-2) receptor tyrosine kinases. The EMBO Journal *15*, 1751.

Kalyankrishna, S., and Grandis, J.R. (2006). Epidermal growth factor receptor biology in head and neck cancer. Journal of Clinical Oncology : Official Journal of the American Society of Clinical Oncology *24*, 2666–2672.

Kamangar, F., Dores, G.M., and Anderson, W.F. (2006). Patterns of cancer incidence, mortality, and prevalence across five continents: defining priorities to reduce cancer disparities in different geographic regions of the world. Journal of Clinical Oncology : Official Journal of the American Society of Clinical Oncology *24*, 2137–2150.

Kawamoto, T., Sato, J.D., Le, a, Polikoff, J., Sato, G.H., and Mendelsohn, J. (1983). Growth stimulation of A431 cells by epidermal growth factor: identification of high-affinity receptors for epidermal growth factor by an anti-receptor monoclonal antibody. Proceedings of the National Academy of Sciences of the United States of America *80*, 1337–1341.

Kelley, D.E., Stokes, D.G., and Perry, R.P. (1999). CHD1 interacts with SSRP1 and depends on both its chromodomain and its ATPase/helicase-like domain for proper association with chromatin. Chromosoma *108*, 10–25.

Keysar, S.B., Le, P.N., Anderson, R.T., Morton, J.J., Bowles, D.W., Paylor, J.J., Vogler, B.W., Thorburn, J., Fernandez, P., Glogowska, M.J., et al. (2013). Hedgehog signaling alters reliance on EGF receptor signaling and mediates anti-EGFR therapeutic resistance in head and neck cancer. Cancer Research Epub ahead of print.

Kimura, H., Sakai, K., Arao, T., Shimoyama, T., Tamura, T., and Nishio, K. (2007). Antibody-dependent cellular cytotoxicity of cetuximab against tumor cells with wild-type or mutant epidermal growth factor receptor. Cancer Science *98*, 1275–1280.

Koutsimpelas, D., Pongsapich, W., Heinrich, U., Mann, S., Mann, W.J., and Brieger, J. (2012). Promoter methylation of MGMT, MLH1 and RASSF1A tumor suppressor genes in head and neck squamous cell carcinoma: pharmacological genome demethylation reduces proliferation of head and neck squamous carcinoma cells. Oncology Reports *27*, 1135–1141.

Kutler, D.I., Auerbach, A.D., Satagopan, J., Giampietro, P.F., Batish, S.D., Huvos, A.G., Goberdhan, A., Shah, J.P., and Singh, B. (2003). High incidence of head and neck squamous cell carcinoma in patients with Fanconi anemia. Archives of Otolaryngology--head & Neck Surgery *129*, 106–112.

Kwak, E.L., Sordella, R., Bell, D.W., Godin-Heymann, N., Okimoto, R. a, Brannigan, B.W., Harris, P.L., Driscoll, D.R., Fidias, P., Lynch, T.J., et al. (2005). Irreversible inhibitors of the EGF receptor may circumvent acquired resistance to gefitinib. Proceedings of the National Academy of Sciences of the United States of America *102*, 7665–7670.

Kyzas, P. a, Stefanou, D., and Agnantis, N.J. (2005a). COX-2 expression correlates with VEGF-C and lymph node metastases in patients with head and neck squamous cell carcinoma. Modern Pathology : an Official Journal of the United States and Canadian Academy of Pathology, Inc *18*, 153–160.

Kyzas, P.A., Cunha, I.W., and Ioannidis, J.P.A. (2005b). Prognostic Significance of Vascular Endothelial Growth Factor Immunohistochemical Expression in Head and Neck Squamous Cell Carcinoma : A Meta-Analysis. Clinical Cancer Research : an Official Journal of the American Association for Cancer Research 1434–1440.

Lee, J.-S., Smith, E., and Shilatifard, A. (2010). The language of histone crosstalk. Cell *142*, 682–685.

Leemans, C.R., Braakhuis, B.J.M., and Brakenhoff, R.H. (2011). The molecular biology of head and neck cancer. Nature Reviews. Cancer *11*, 9–22.

Lichtenberger, B.M., Tan, P.K., Niederleithner, H., Ferrara, N., Petzelbauer, P., and Sibilia, M. (2010). Autocrine VEGF signaling synergizes with EGFR in tumor cells to promote epithelial cancer development. Cell *140*, 268–279.

Liang, L., Li, Y., and Tollefsbol, T. (2008). Gene-environment interactions and epigenetic basis of human diseases. Curr Issues Mol Biol *10*, 25–36.

Lujambio, A., and Esteller, M. (2009). How epigenetics can explain human metastasis: a new role for microRNAs. Cell cycle *8,* 377–382.

Melillo, G. (2007). Targeting hypoxia cell signaling for cancer therapy. Cancer Metastasis Reviews *26*, 341–352.

Metzker, M.L. (2010). Sequencing technologies - the next generation. Nature Reviews Genetics *11*, 31–46.

Morgillo, F., Bareschino, M.A., Bianco, R., Tortora, G., and Ciardiello, F. (2007). Primary and acquired resistance to anti-EGFR targeted drugs in cancer therapy. Differentiation; Research in Biological Diversity *75*, 788–799.

Olsson, A.-K., Dimberg, A., Kreuger, J., and Claesson-Welsh, L. (2006). VEGF receptor signalling - in control of vascular function. Nature Reviews. Molecular Cell Biology *7*, 359–371.

Pao, W., Miller, V. a, Politi, K. a, Riely, G.J., Somwar, R., Zakowski, M.F., Kris, M.G., and Varmus, H. (2005). Acquired resistance of lung adenocarcinomas to gefitinib or erlotinib is associated with a second mutation in the EGFR kinase domain. PLoS Medicine *2*, e73.

Pries, R., Hogrefe, L., Lei, X., Frenzel, H., Brocks, C., DITZ, C., and WOLLENBERG, B. (1998). Induction of c-Myc-dependent cell proliferation through toll-like receptor 3 in head and neck cancer. International Journal of Molecular Medicine *21*, 209–215.

Ragin, C.C.R., Modugno, F., and Gollin, S.M. (2007). The Epidemiology and Risk Factors of Head and Neck Cancer: a Focus on Human Papillomavirus. Journal of Dental Research *86*, 104–114.

Reis-Filho, J.S. (2009). Next-generation sequencing. Breast Cancer Research : BCR *11 Suppl 3*, S12.

Rosenzweig, S. a (2012). Acquired resistance to drugs targeting receptor tyrosine kinases. Biochemical Pharmacology *83*, 1041–1048.

Roskoski, R. (2004). The ErbB/HER receptor protein-tyrosine kinases and cancer. Biochemical and Biophysical Research Communications *319*, 1–11.

Rubin Grandis, J., Melhem, M.F., Barnes, E.L., and Tweardy, D.J. (1996). Quantitative immunohistochemical analysis of transforming growth factor-alpha and epidermal growth factor receptor in patients with squamous cell carcinoma of the head and neck. Cancer *78*, 1284–1292.

Rygaard, J., and Poulsen, C.O. (2009). HETEROTRANSPLANTATION OF A HUMAN MALIGNANT TUMOUR TO "NUDE" MICE. Acta Pathologica Microbiologica Scandinavica *77*, 758–760.

Schlessinger, J. (2002). Dimerization and Activation of EGF Receptor. *110*, 669–672.

Schotta, G., Ebert, A., Krauss, V., Fischer, A., Hoffmann, J., Rea, S., Jenuwein, T., Dorn, R., and Reuter, G. (2002). Central role of Drosophila SU(VAR)3-9 in histone H3-K9 methylation and heterochromatic gene silencing. The EMBO Journal *21*, 1121–1131.

Scully, C., and Bagan, J. (2009). Oral squamous cell carcinoma overview. Oral Oncology *45*, 301–308.

Sharif, A., and Prevot, V. (2010). ErbB receptor signaling in astrocytes: a mediator of neuron-glia communication in the mature central nervous system. Neurochemistry International *57*, 344–358.

Sibilia, M., Fleischmann, a, Behrens, a, Stingl, L., Carroll, J., Watt, F.M., Schlessinger, J., and Wagner, E.F. (2000). The EGF receptor provides an essential survival signal for SOS-dependent skin tumor development. Cell *102*, 211–220.

Sibilia, M., Kroismayr, R., Lichtenberger, B.M., Natarajan, A., Hecking, M., and Holcmann, M. (2007). The epidermal growth factor receptor: from development to tumorigenesis. Differentiation; Research in Biological Diversity *75*, 770–787.

Smith, A., Teknos, T.N., and Pan, Q. (2013). Epithelial to mesenchymal transition in head and neck squamous cell carcinoma. Oral Oncology *49*, 287–292.

Squarize, C.H., Castilho, R.M., Giudice, F.S., and No, J.E. (2013). Inhibition of Histone Deacetylase Impacts Cancer Stem Cells and Induces Epithelial-Mesenchyme Transition of Head and Neck Cancer. *8*.

Ting, A.H., McGarvey, K.M., and Baylin, S.B. (2006). The cancer epigenome--components and functional correlates. Genes & Development *20*, 3215–3231.

Twigger, K., Roulstone, V., Kyula, J., Karapanagiotou, E.M., Syrigos, K.N., Morgan, R., White, C., Bhide, S., Nuovo, G., Coffey, M., et al. (2012). Reovirus exerts potent oncolytic effects in head and neck cancer cell lines that are independent of signalling in the EGFR pathway. BMC Cancer *12*, 368.

Verma, M., Seminara, D., Arena, F.J., John, C., Iwamoto, K., and Hartmuller, V. (2006). Genetic and epigenetic biomarkers in cancer : improving diagnosis, risk assessment, and disease stratification. Molecular Diagnosis & Therapy *10*, 1–15.

Viloria-petit, A., and Kerbel, R.S. (2004). Acquired resistance to EGFR inhibitors: mechanisms and prevention strategies. International Journal of radiation oncology *58,* 914-926.

Viloria-petit, A., Crombet, T., Jothy, S., Angiogenesis, T., Hicklin, D., Bohlen, P., Schlaeppi, J.M., Rak, J., and Kerbel, R.S. (2001). Acquired Resistance to the Antitumor Effect of Epidermal Growth Factor Receptor-blocking Antibodies in Vivo : A Role for Altered Tumor Angiogenesis. Cancer research *61*, 5090–5101.

Waddington, C.H. (2012). The epigenotype. 1942. International Journal of Epidemiology *41*, 10–13.

Weber, A., Wittekind, C., and Tannapfel, A. (2003). Genetic and epigenetic alterations of 9p21 gene products in benign and malignant tumors of the head and neck. Pathology, Research and Practice *199*, 391–397.

Weber, A., Dietz, A., Tischoff, I., and Tannapfel, A. (2007). [Role of epigenetics in the carcinogenesis of head and neck carcinomas - possible new targeted therapy?]. Laryngo-Rhino- Otologie *86*, 9–13.

Wheeler, D.L., Madison, H.A., and Harari, P.M. (2010). Understanding resistance to EGFR inhibitors-impact on future treatment strategies. Nature reviews. Clinical oncology *7*, 493–507.

Wu, S.C., and Zhang, Y. (2010). Active DNA demethylation: many roads lead to Rome. Nature Reviews. Molecular Cell Biology *11*, 607–620.

Yamasaki, F., Johansen, M.J., Zhang, D., Krishnamurthy, S., Felix, E., Bartholomeusz, C., Aguilar, R.J., Kurisu, K., Mills, G.B., Hortobagyi, G.N., et al. (2007). Acquired resistance to erlotinib in A-431 epidermoid cancer cells requires down-regulation of MMAC1/PTEN and up-regulation of phosphorylated Akt. Cancer Research *67*, 5779–5788.

Yarden, Y., and Sliwkowski, M.X. (2001). Untangling the ErbB signalling network. Nature Reviews. Molecular Cell Biology *2*, 127–137.

Zhao, F.Y., Shao, C.P., Li, Y., Ma, W.Y., Tian, N., and Zheng, J.H. (2013). 5-Azacytidine induces early stage apoptosis and promotes in vitro maturation by changing chromosomal construction in murine oocytes. Reproductive Toxicology (Elmsford, N.Y.) *37*, 56–61.

Zimmermann, M., Zouhair, A., Azria, D., and Ozsahin, M. (2006). The epidermal growth factor receptor (EGFR) in head and neck cancer: its role and treatment implications. Radiation Oncology (London, England) *1*, 11.

7 Appendix

7.1 Abstract

The epidermal growth factor receptor (EGFR) is a critical regulator of the self-renewal and differentiation of epidermal cells and is commonly expressed at high levels in a variety of epithelial tumors. Head and neck squamous cell carcinoma (HNSCC) is a distinct cancer type, in which the EGFR has been shown to be overexpressed in up to 100% of cases. This type of cancer is the sixth most common malignant tumor world-wide and responsible for approximately 350,000 deaths annually. Due to the deregulation of EGFR signaling in pre-stage HNSCC, the EGFR is a preferential target for novel therapies, with a broad spectrum of inhibitors being currently under investigation. One such drug, approved by the Food and Drug Administration (FDA), is cetuximab, a monoclonal antibody which inhibits EGFR dimerization and is successfully used in the treatment against cancer. Many patients initially respond well to the treatment, but later on develop a resistance against the drug, which ultimately leads to relapse. Hence, efforts are needed to better understand the mechanisms leading to acquired resistance as well as strategies to overcome it. In this thesis, two squamous cell carcinoma cell lines, one head and neck carcinoma cell line (HNSCC22) and one squamous cell carcinoma cell line (SCC13) were induced to develop resistance to cetuximab. Subsequently, these cell lines were characterized for the molecular changes accompanying loss of cetuximab-sensitivity. No increased late-stage apoptosis was detected in cetuximab-sensitive cells upon exposure to the drug for 48 h. Quantitative proliferation analysis revealed a significant decrease after exposure to cetuximab for 48 h in the cell line SCC13 S. Furthermore, treatment with cetuximab resulted in decreased phosphorylation of the extracellular signal-regulated kinases 1 and 2 (ERK1/2) in a dose-dependent manner in sensitive cell lines, whereas no effect was seen in cetuximab-resistant cell lines. Moreover, all cell lines retained their proliferative potential *in vivo*, although there were no significant differences in the size of orthotopic tumors derived from sensitive and resistant cell lines. Next generation sequencing (NGS) demonstrated that there were no global differences in DNA methylation between the sensitive and resistant cells. However, changes in the expression of various chromatin remodeling factors as well as of genes involved in the VEGF pathway could be detected. Surprisingly, simultaneous exposure to cetuximab and VEGF revealed that VEGF increased the inhibitory effect of cetuximab on cancer cells.

In summary, I have generated cetuximab-resistant human (HN)SCC cell lines and analyzed their properties by various approaches. By performing NGS, I analyzed the methylomes and transcriptomes of cetuximab-resistant and –sensitive cell lines and could find a deregulation of several genes. The analysis of VEGF, as a potent candidate gene, gave us an interesting hint about its potential use to increase cetuximab-sensitivity in HNSCC. This model provides an important preclinical tool to investigate molecular mechanisms of acquired resistance to EGFR blockade and to specify candidate genes involved in acquired resistance, which may be useful as biomarkers.

7.2 Zusammenfassung

Der epidermale Wachstumsfaktor-Rezeptor (EGFR) ist ein wichtiger Regulator der Selbsterneuerung und Differenzierung von Zellen der Epidermis und wird häufig in hohen Konzentrationen in einer Vielzahl von epithelialen Tumoren exprimiert. Das Plattenepithelkarzinom im Kopf-Hals-Bereich ist eine bestimmte Krebsart, in der der EGFR in bis zu 100% der Fälle überexprimiert wird. Diese Art von Krebs ist der sechsthäufigste bösartige Tumor weltweit und verantwortlich für etwa 350.000 Todesfälle pro Jahr. Aufgrund der Deregulierung des EGFR-Signalwegs in Vorstufen von Plattenepithelkarzinomen des Kopf-Hals-Bereichs, ist er ein bevorzugter Ansatzpunkt für neuartige Therapien mit einem breiten Spektrum an Inhibitoren, die derzeit untersucht werden. Cetuximab, ein monoklonaler Antikörper, der die EGFR Dimerisierung verhindert, wurde durch die „Food and Drug Administration" (FDA) genehmigt und erfolgreich in der Behandlung gegen Krebs eingesetzt. Viele Patienten sprechen anfänglich gut auf das Medikament an, entwickeln jedoch im weiteren Behandlungsverlauf eine Resistenz, was schließlich zu Rückfällen führt. Daher ist es notwendig, die Mechanismen, die zur erworbenen Resistenz führen sowie die Strategien, diese zu überwinden, besser zu verstehen. Für diese Arbeit wurden zwei Plattenepithelkarzinom-Zelllinien, eine Kopf- und Hals-Karzinom-Zelllinie (HNSCC22) sowie eine epidermale Plattenepithelkarzinom-Zelllinie (SCC13) induziert, um eine Resistenz gegen Cetuximab zu entwickeln. Anschließend wurden die molekularen Veränderungen der Zelllinien, die mit dem Verlust der Cetuximab-Sensitivität einhergehen, charakterisiert. Es wurde kein erhöhtes Spätstadium von Apoptose in Cetuximab-sensitiven Zelllinen bei Einwirkung des Medikamentes für 48 h nachgewiesen. Eine quantitative Proliferationsanalyse zeigte einen signifikanten Rückgang nach der Exposition gegenüber Cetuximab für 48 h in der Zelllinie SCC13 S. Zudem führte die Behandlung mit Cetuximab zu einer Dosis-abhängigen Verringerung der Phosphorylierung der extrazellulär-signalregulierten Kinasen 1 und 2 (ERK1/2) in den Cetuximab-sensitiven Zelllinien, wohingegen kein Effekt in Cetuximab-resistenten Zelllinien sichtbar war. Darüber hinaus erhielten alle Zelllinien ihr proliferatives Potential *in vivo*, obwohl keine signifikanten Unterschiede in der Größe der orthotopen Tumoren von sensitiven und resistenten Zelllinien festgestellt werden konnte. Die Sequenzierung der nächsten Generation (NGS) zeigte, dass es keine Unterschiede in der globalen DNA Methylierung zwischen den sensitiven und resistenten Zellen gab. Jedoch

konnten Änderungen in der Expression verschiedener Chromatin-Remodellierungs-Faktoren sowie von Genen, die im VEGF Signalweg beteiligt sind, nachgewiesen werden. Überraschenderweise zeigte eine gleichzeitige Behandlung mit Cetuximab und VEGF, dass VEGF die hemmende Wirkung von Cetuximab auf Krebszellen erhöht.

Zusammenfassend habe ich Cetuximab-resistente humane Zelllinien generiert und ihre Eigenschaften durch unterschiedliche Methoden charakterisiert. Mit der Durchführung von NGS habe ich die Methylome und Transkriptome von Cetuximab-resistenten und – sensitiven Zelllinien analysiert, wobei ich eine Deregulierung von mehreren Genen zeigen konnte. Die Analyse von VEGF, als ein potentielles „Kandidaten-Gen", gab uns einen interessanten Hinweis über die mögliche Verwendung von VEGF, um die Empfindlichkeit von (HN)SCC Zelllinien gegenüber Cetuximab zu erhöhen. Dieses Modell stellt ein wichtiges präklinisches Werkzeug dar, um molekulare Mechanismen der erworbenen Resistenz gegenüber der EGFR-Blockade zu untersuchen und um „Kandidaten-Gene" zu erkennen, die ebenfalls als Biomarker Verwendung finden können.

7.3 List of Figures

7.4 List of Tables

7.5 List of Abbreviations

7´AAD	7´actinoaminomycin
A	adenosine
C	cytosine
°C	degree Celsius
cDNA	complementary DNA
cet	cetuximab
CpG	poly-cytosine poly-guanosine
ctrl	control
ddH$_2$O	double-distilled water (cell culture water)
DMEM	Dulbecco´s Modified Eagle´s Medium
DMSO	dimethyl sulfoxide
DNA	desoxyribonucleic acid
dNTP	desoxyribonucleosid-5´-triphosphate
EGFR	epidermal growth factor receptor
et al.	and others (*et alii*)
FBS	fetal bovine serum
g	gram
G	guanosine
HNSCC	head and neck squamous cell carcinoma
HPV	human papillomavirus
hr	hour
IC$_{50}$%	half maximal inhibitory concentration
kb	kilo base
l	liter
min	minute
M	mol
mg	milligram
ml	milliliter
mM	millimol
mRNA	*messenger* RNA
µg	microgram
µl	microliter
µM	micromole
NaCl	sodium chloride
NFW	nuclease free water

nM	nanomol
o/n	overnight
PBS	phosphate buffered saline
PCR	polymerase chain reaction
Pen/Strep	penicillin/streptomycin
qRT-PCR	quantitative real-time PCR
R	resistant
RNA	ribonucleic acid
rpm	rounds per minute
RT	room temperature
RT	radiation therapy
S	sensitive
SCC	squamous cell carcinoma
SD	standard deviation
SDS	sodium dodecylsulfate
sec	second
ss	single stranded
T	thymidine
TGF-α	transforming growth factor alpha
TKI	tyrosine-kinase inhibitor
VEGF	vascular endothelial growth factor
w/o	without

7.6 Curriculum Vitae

Education:

Course of studies:	2010 –	Master of Science in Molecular Microbiology and Immunology at the University of Vienna
	2007 – 2010	Bachelor of Science in Biology at the University of Göttingen passed with distinction
Secondary school:	2007	final secondary school examinations at Campe-Gymnasium, 37603 Holzminden
	2000 – 2007	Campe-Gymnasium, 37603 Holzminden
	1998 – 2000	Orientierungsstufe, 37632 Eschershausen
Elementary school:	1997 – 1998	Grundschule, 37632 Eschershausen
	1994 – 1997	Grundschule am Nordsolling, 37627 Deensen
	1994 – 1994	Gustav-Sieber-Grundschule, 71732 Tamm

Additional skills

Language:	German (native), French (basic), English (fluent, UNIcert III Scientific English)
IT:	proficient in Microsoft Office, advanced in GraphPad Prism